The neutron double differential cross-section of simple molecular fluids: refined computing models and nowadays applications

2003 J. Phys.: Condens. Matter 15 R775

(http://iopscience.iop.org/0953-8984/15/19/204)

INSTITUTE OF PHYSICS PUBLISHING JOURNAL OF PHYSICS: CONDENSED MATTER

J. Phys.: Condens. Matter **15** (2003) R775–R812 PII: S0953-8984(03)58810-5

TOPICAL REVIEW

The neutron double differential cross-section of simple molecular fluids: refined computing models and nowadays applications

Eleonora Guarini

Istituto Nazionale per la Fisica della Materia, Unità di Ricerca di Firenze, via G Sansone 1, I-50019 Sesto Fiorentino, Italy

Received 27 January 2003
Published 6 May 2003
Online at stacks.iop.org/JPhysCM/15/R775

Abstract

A review of the available tools for the calculation of the neutron double-differential cross-section of fundamental molecules, such as hydrogen and methane, is reported here. The most common cases occurring in neutron data analysis are treated in detail with the aim of providing the reader with intelligible and efficient procedures. The utility nowadays of these kinds of computation are widely described, and applications discussed, with examples based on the comparison with experimental data. New advances and refinement/corrections of earlier work are given throughout the paper, as well as suggestions for practical implementation.

Contents

0953-8984/03/190775+38$30.00

1. Introduction

More than 50 years of research have been devoted to the development of calculation methods and models able to describe the scattering of slow and thermal neutrons from simple molecular systems, [1–19] representing only part of the huge work on the subject. Most studies on the dynamical response to neutrons of light molecular gases and liquids—mainly hydrogen and methane—were stimulated, beyond their fundamental physical significance, by important applications in the field of neutron science and technology (e.g. moderators in neutron sources, cold neutron sources, neutron shielding, etc).

As a matter of fact, the general interest in the refinement of models for the computation of the neutron differential cross-sections (either *self* or *distinct*, or both, as explained in the following sections) of simple molecules such as hydrogen, methane, their heavy counterparts (D_2, CD_4) and, to some approximation, of other di- and polyatomic fluids, has never faded through the years. This is partly due to the experimental work devoted, in the last decade and at present, to the accurate determination of the microscopic static structure of quantum and classical molecular fluids by neutron diffraction techniques [19–25], which requires both a reasonable evaluation of the inelastic contributions to the scattered intensity and a good modelling of the intra- and intermolecular neutron cross-sections, necessary to allow for the extraction of the centre-of-mass (CM) structure factor of the measured samples. Another, equally important, reason for such a reiterated concern is the rather modern introduction of dilute H_2 and CH_4 as competing (with respect to vanadium or water) normalization standards for neutron diffraction experiments on liquid and gaseous samples [26–28], which relies on the use of accurate models—including a quantum mechanical treatment of rotations and vibrations—for the *self*-differential cross-section of low-density hydrogen or methane, at various incident neutron energies and over different wavevector transfer ranges, depending on the experimental circumstances.

The present need for well-established procedures to calculate the neutron differential cross-sections of the quoted molecular systems and, particularly, for the effective tools and simple knowledge useful in related computer programming and implementation, is not fully supported, however, by the available literature. Indeed, papers on this subject often have a heavily theoretical cut, and suffer either from the rather complex, but unavoidably concise, exposition of the basic theory and approximations, or from continuously mismatched notation, which is sometimes difficult to follow from one paper to another. In addition, several misprints or incomplete formulae can be detected by careful inspection of theories and quantum-mechanical calculations in the literature, which should definitely be reported and settled, in order to prevent their inadvertent use.

One of the aims of this paper is therefore to translate (and gather) for *true users* the essence of a huge amount of theoretical work on neutron cross-sections of simple molecules. As far as possible, a self-consistent picture of the calculations required will be given. Basic formulae, easily applicable to practical computation and computer programming, will be explained and reported, together with a description of the approximations, and some advice concerning

numerical problems or useful tricks. Preliminary checks, necessary to assess the computational requirements, will also be described in some detail.

Another objective of this work is to give the reader a unified, improved and updated reference for this field, including examples, corrections and/or extensions of previous papers, comparison with recent experimental results when possible, and mention of still open problems. Of course, several original contributions are reported also. The case of the hydrogens (H_2 and D_2) will be discussed, as well as that of methane (CH_4 and CD_4). For the latter, a smooth quantum-mechanical calculation, also allowing for the treatment of the lowest vibrational transitions, is proposed here and tested against experimental data. Approximate model calculations for chlorine will be described as well.

2. The neutron double-differential cross-section of molecular fluids: review

Consider the scattering of slow and thermal neutrons from a system composed of N identical polyatomic molecules, each containing n nuclei. If the neutron momentum changes from $\hbar\boldsymbol{k}_0$ to $\hbar\boldsymbol{k}_1$ during a collision with an energy transfer $E = E_0 - E_1$, while the molecular system simultaneously undergoes a transition between an initial (global, i.e. vibro-roto-translational-spin) state $|L_0\rangle$ of energy E_{L_0}, and a final (global) state $|L_1\rangle$ of energy E_{L_1}, then the double-differential cross-section per molecule (per unit solid angle and unit energy transfer) can be written as

$$\frac{\mathrm{d}^2\sigma}{\mathrm{d}\Omega\,\mathrm{d}E} = \frac{1}{N}\frac{k_1}{k_0}\sum_{L_0\mu_0} p_{L_0}p_{\mu_0}\sum_{L_1\mu_1}|\langle\mu_1|\langle L_1|\sum_{j=1}^{N}\sum_{\nu=1}^{n}\hat{b}_{j\nu}\mathrm{e}^{\mathrm{i}\boldsymbol{Q}\cdot\boldsymbol{R}_{j\nu}}|L_0\rangle|\mu_0\rangle|^2\delta(E+E_{L_0}-E_{L_1}) \tag{1}$$

where $|\mu_0\rangle$ and $|\mu_1\rangle$ synthetically represent the initial and final spin states of the neutron $|1/2\ \mu\rangle$, with μ the quantum number of the z component of the neutron spin operator; $\boldsymbol{Q} = \boldsymbol{k}_0 - \boldsymbol{k}_1$ is the wavevector transfer; $\boldsymbol{R}_{j\nu}$ and $\hat{b}_{j\nu}$ are, respectively, the position vector and scattering length operator (depending on both the spin $\boldsymbol{I}_{j\nu}$ of the nucleus and the spin $\boldsymbol{s}$ of the neutron) of the νth nucleus in the jth molecule; p_{L_0} and p_{μ_0} indicate the probability of the initial states $|L_0\rangle$ and $|\mu_0\rangle$; and the Dirac delta function accounts for the conservation of the total energy, i.e. $E_{L_0} + E_0 = E_{L_1} + E_1$, in the process. Equation (1) is simply the generalization to molecules of the well-known *master formula* of neutron scattering (see, e.g., [17, 29]), when the Fermi pseudopotential is used as the neutron–nucleus interaction. The above equation is valid (i) within the limits of the first Born approximation, (ii) if no electronic transition is allowed in the scattering event, and (iii) if the adiabatic approximation for the electronic motion holds, with the molecules permanently remaining in their ground electronic state.

In order to facilitate the comparison with many experimental papers, it is preferable to change the energy variables according to $E = \hbar\omega$, and to rewrite equation (1) in the form

$$\frac{\mathrm{d}^2\sigma}{\mathrm{d}\Omega\,\mathrm{d}\omega} = \frac{1}{2\pi N}\frac{k_1}{k_0}\int \mathrm{d}t\ \mathrm{e}^{-\mathrm{i}\omega t}\sum_{L_0\mu_0} p_{L_0}p_{\mu_0}\sum_{L_1\mu_1}\mathrm{e}^{\mathrm{i}\omega_{L_0L_1}t}|\langle\mu_1|\langle L_1|\sum_{j=1}^{N}\sum_{\nu=1}^{n}\hat{b}_{j\nu}\mathrm{e}^{\mathrm{i}\boldsymbol{Q}\cdot\boldsymbol{R}_{j\nu}}|L_0\rangle|\mu_0\rangle|^2 \tag{2}$$

where the integral representation of the Dirac delta function was used and $\omega_{L_0L_1} = (E_{L_1} - E_{L_0})/\hbar$. The position vector $\boldsymbol{R}_{j\nu}$ can, of course, be expressed as $\boldsymbol{R}_{j\nu} = \boldsymbol{R}_j + \boldsymbol{r}_{j\nu}$, that is as the sum of the position vector $\boldsymbol{R}_j$ of the CM of the molecule and the position vector $\boldsymbol{r}_{j\nu}$, with respect to the CM, of nucleus ν inside the molecule itself.

In what follows, we shall make the basic assumption that the *simple* (i.e. insulating and highly symmetric) molecules we are interested in behave as *free vibro-rotors*. This

means that the intermolecular interactions are ruled by an essentially isotropic potential, and that the relative orientations of the molecules (rotation coupling), as well as the coupling between vibrational states of different molecules, play a negligible role. As a consequence, the translational (CM) dynamics of the molecules in the system can be considered as completely independent of the individual roto-vibrational states. Such an assumption is known to be justified even for the solid (low-pressure) phase of the hydrogens [30], and can represent a reasonable starting point for heavier homonuclear diatomic molecules, whenever the anisotropic contributions are treatable as small perturbations of the isotropic intermolecular potential. Concerning methane, the validity of the free-rotor approximation arises from [15]: (i) its high symmetry, (ii) the absence of molecular clustering phenomena, even at liquid densities, and (iii) experimental evidence of weak intermolecular rotational correlations [31], i.e. negligible orientation-dependent interactions.

For free rotors, the global state $|L\rangle$ can thus be factorized as $|L\rangle = |\tau\rangle|W\rangle$, where $|\tau\rangle$ is the complete set representing the overall translational state of the system and $|W\rangle$ is its roto-vibrational and spin state. Note that the latter definitions mean also that the CM translational dynamics is independent of the molecular spin states. The new version of equation (2) resulting from the above quoted assumptions is

$$\begin{aligned}\frac{\mathrm{d}^2\sigma}{\mathrm{d}\Omega\,\mathrm{d}\omega} = \frac{1}{2\pi N}\frac{k_1}{k_0}\int \mathrm{d}t\,\mathrm{e}^{-\mathrm{i}\omega t}\sum_{i,j=1}^{N}\sum_{\tau_0\tau_1} p_{\tau_0}\mathrm{e}^{\mathrm{i}\omega_{\tau_0\tau_1}t}\langle\tau_0|\mathrm{e}^{-\mathrm{i}\boldsymbol{Q}\cdot\boldsymbol{R}_i}|\tau_1\rangle\langle\tau_1|\mathrm{e}^{\mathrm{i}\boldsymbol{Q}\cdot\boldsymbol{R}_j}|\tau_0\rangle \\ \times \sum_{W_0\mu_0} p_{W_0}p_{\mu_0}\sum_{W_1\mu_1}\mathrm{e}^{\mathrm{i}\omega_{W_0W_1}t}\langle\mu_0|\langle W_0|\sum_{v=1}^{n}\hat{b}_{iv}^{*}\mathrm{e}^{-\mathrm{i}\boldsymbol{Q}\cdot\boldsymbol{r}_{iv}}|W_1\rangle|\mu_1\rangle\langle\mu_1|\langle W_1| \\ \times \sum_{v'=1}^{n}\hat{b}_{jv'}\mathrm{e}^{\mathrm{i}\boldsymbol{Q}\cdot\boldsymbol{r}_{jv'}}|W_0\rangle|\mu_0\rangle. \qquad (3)\end{aligned}$$

By using the completeness relation over the translational states and expressing the centre-of-mass position operators in the Heisenberg representation, the double-differential cross-section can be rewritten in terms of the *self* and *distinct* intermediate scattering functions, $F_s(\boldsymbol{Q},t) = \frac{1}{N}\sum_{i=1}^{N}\langle\mathrm{e}^{-\mathrm{i}\boldsymbol{Q}\cdot\boldsymbol{R}_i(0)}\mathrm{e}^{\mathrm{i}\boldsymbol{Q}\cdot\boldsymbol{R}_i(t)}\rangle$ and $F_d(\boldsymbol{Q},t) = \frac{1}{N}\sum_{\substack{i,j=1\\ i\neq j}}^{N}\langle\mathrm{e}^{-\mathrm{i}\boldsymbol{Q}\cdot\boldsymbol{R}_i(0)}\mathrm{e}^{\mathrm{i}\boldsymbol{Q}\cdot\boldsymbol{R}_j(t)}\rangle$, as

$$\begin{aligned}\frac{\mathrm{d}^2\sigma}{\mathrm{d}\Omega\,\mathrm{d}\omega} = \frac{1}{2\pi}\frac{k_1}{k_0}\int \mathrm{d}t\,\mathrm{e}^{-\mathrm{i}\omega t}[F_s(Q,t)v(Q,t) + F_d(Q,t)u(Q)] \\ \text{with } v(Q,t) = \sum_{w_0\mu_0} p_{w_0}p_{\mu_0}\sum_{w_1\mu_1}\mathrm{e}^{\mathrm{i}\omega_{w_0w_1}t}|\langle\mu_1|\langle w_1|\hat{O}|w_0\rangle|\mu_0\rangle|^2 \\ \text{and } u(Q) = \sum_{\mu_0} p_{\mu_0}\sum_{\mu_1}\left|\sum_{w_0} p_{w_0}\langle\mu_1|\langle w_0|\hat{O}|w_0\rangle|\mu_0\rangle\right|^2 \qquad (4)\end{aligned}$$

where $\hat{O} = \sum_{v=1}^{n}\hat{b}_v\mathrm{e}^{\mathrm{i}\boldsymbol{Q}\cdot\boldsymbol{r}_v}$ is a single-molecule operator and we have used the factorization $|W\rangle = |w\rangle^{(1)}|w\rangle^{(2)}\cdots|w\rangle^{(N)}$ into N single-molecule (roto-vibrational and spin) states. Therefore, both $u(Q)$ and $v(Q,t)$ are single-molecule functions, and it should be clear that equation (4) only holds for a system of N strictly *identical* molecules, i.e. with exactly the same isotopic composition. Since $u(Q)$ is time-independent, the distinct part in equation (4) reduces to $(\frac{\mathrm{d}^2\sigma}{\mathrm{d}\Omega\,\mathrm{d}\omega})_d = \frac{k_1}{k_0}u(Q)S_d(Q,\omega)$, which probes the intermolecular CM dynamics of the fluid arising from correlations (ruled by the interaction potential) between different molecules. Note that the van Hove coherent–incoherent description of the dynamic structure factor corresponds, in the self-distinct formalism, to $S(Q,\omega) = S_{coh}(Q,\omega) = S_d(Q,\omega) + S_s(Q,\omega)$, while $S_{inc}(Q,\omega) = S_s(Q,\omega)$. Purely coherent scattering will thus characterize $u(Q)$ and, consequently, the distinct contribution to the total cross-section. Concerning the intramolecular

structure, i.e. the self part in equation (4), it is seen that, at the present stage, the time dependence of $v(Q,t)$ prevents one from deriving an explicit expression in terms of the self dynamic structure factor $S_s(Q,\omega) = \frac{1}{2\pi}\int \mathrm{d}t\, \mathrm{e}^{-\mathrm{i}\omega t} F_s(Q,t)$. However, by noting that time enters the expression of $v(Q,t)$ only in exponential form, it is possible to rewrite the self part of equation (4) as

$$\begin{aligned}\left(\frac{\mathrm{d}^2\sigma}{\mathrm{d}\Omega\,\mathrm{d}\omega}\right)_s &= \frac{1}{2\pi}\frac{k_1}{k_0}\sum_{w_0\mu_0 w_1\mu_1} p_{w_0}p_{\mu_0}\left|\langle\mu_1|\langle w_1|\sum_{v=1}^{n}\hat{b}_v\,\mathrm{e}^{\mathrm{i}\boldsymbol{Q}\cdot\boldsymbol{r}_v}|w_0\rangle|\mu_0\rangle\right|^2 \\ &\quad\times\int \mathrm{d}t\,\mathrm{e}^{-\mathrm{i}\omega t}\,\mathrm{e}^{\mathrm{i}\omega_{w_0w_1}t}F_s(Q,t) \\ &= \frac{k_1}{k_0}\sum_{w_0\mu_0 w_1\mu_1} p_{w_0}p_{\mu_0}\left|\langle\mu_1|\langle w_1|\sum_{v=1}^{n}\hat{b}_v\,\mathrm{e}^{\mathrm{i}\boldsymbol{Q}\cdot\boldsymbol{r}_v}|w_0\rangle|\mu_0\rangle\right|^2 S_s(Q,\omega-\omega_{w_0w_1}). \qquad (5)\end{aligned}$$

Thus, the overall self part corresponds to the sum, over the possible transitions, of single-molecule contributions in which the translational self dynamics can effectively be factored out, but explicitly depends (through a frequency shift) on the specific intramolecular transition. Transition probabilities are also seen to rule the importance of the various terms in the above series.

Equation (4) quite generally represents the starting point for these kinds of calculations, which, apart from the problem of choosing appropriate models for the self and distinct translational dynamics (addressed in the remainder of this paper), deals firstly with the calculation of $u(Q)$ and $v(Q,t)$.

In this respect, the next fundamental point in computing $u(Q)$ and $v(Q,t)$ for the systems we are mainly concerned with in this paper, that is the homonuclear diatomic and the spherical-top molecules, depends on whether the effects of nuclear spin statistics can or cannot be neglected. Unless nuclei of the same element present in the molecule can be treated as Boltzmann particles (i.e. quantum effects related to the indistinguishability principle can be neglected, either because of the high temperature or because identical nuclei have spin $I \to \infty$) the symmetry requirements on the total molecular wavefunction impose a coupling between the total spin state and the rotational state of the molecule (assumed to be in the ground vibrational state). Such a coupling, widely addressed as a 'spin correlation', not only alters the multiplicity of the rotational levels with respect to the uncorrelated case, but the way in which this modification takes place *changes* with the specific rotational state under consideration (see, e.g., [32]). This affects the resulting cross-section, since the initial state probabilities p_{w_0} turn out to depend on the present species concentrations (ortho, para, meta ...) and the expressions change, in general, when the rotational level is varied. Further, the spin dependence of the neutron scattering length operator, namely $\hat{b} = b_{coh} + \frac{2b_{inc}}{\sqrt{I(I+1)}}\boldsymbol{s}\cdot\boldsymbol{I}$, has peculiar effects on the scattering cross-section when spin correlations are taken into account. In fact, the rotational transitions induced by the neutrons are found to be weighted by different (sometimes leading to very different values) combinations of b_{coh} and b_{inc}, depending on the specific levels involved.

In the case of the hydrogens, e.g. [9, 10, 13, 19], spin correlation effects are particularly important, but fortunately, as for all homonuclear diatomic molecules, they are ruled only by the *parity* of the rotational states (and not by the specific rotational quantum numbers). Moreover, only one species (ortho or para) can occur for a given rotational level of a diatomic molecule. Such simplifications, however, do not apply to other molecules, like spherical tops and symmetric tops, where more than one species can coexist for a given rotational state and no easy (e.g. parity-dependent) rule can be derived in order to account for spin correlation effects on the rotational levels degeneracy [32]. A careful treatment of spin correlations for the methane molecule [12] has shown, however, that their effects on the scattering response

become appreciable only for the gas at very low temperatures (∼10 K), which is a rather atypical condition for common applications, usually regarding either gaseous methane at room temperature (e.g. for neutron data normalization purposes) or liquid methane near to the triple point (∼100 K, e.g. in the case of neutron moderators).

A reasonable criterion for choosing whether to carry out the uncorrelated-spin case or not is to compare the rotational constant B of the molecule with the thermal energy for the case of interest (k_BT, with k_B the Boltzmann constant) [13, 15]. In the 'high temperature limit', $k_BT \gg B$, quantum effects due to indistinguishability of the nuclei are expected to vanish and the resulting cross-section is that of Boltzmann particles. According to this criterion, it is seen that the lighter and smaller is the molecule (the larger is B), the higher are the temperatures at which the neglect of spin correlations starts to be admissible. Hydrogen is liquid down to very low temperatures (∼20 K) compared to other molecular liquids such as methane (∼90 K). In addition, the rotational constant of hydrogen (7.35 meV) is the highest among molecules (for instance, $B = 0.65$ meV for methane). Therefore, while nuclear spin statistics and correlations deeply characterize the shape of the neutron spectra from the hydrogens in most thermodynamic states, the same does not happen for other molecules, even at their liquid temperatures.

In the next subsections we shall consider the homonuclear diatomic molecules, both in the presence of spin correlations and in the uncorrelated case. The latter will also be carried out for the more complicated situation of spherical-top molecules. It is useful to note by now that, when spin correlations are neglected, the states W in equation (3) can be further factorized into $|W\rangle = |S\rangle|U\rangle$, where $|S\rangle$ represents the total molecular spin state of the system and $|U\rangle$ the total roto-vibrational state. The large simplification in the uncorrelated case lies in the fact that summations over matrix elements involving spin variables (contained in the scattering length operators) and those related to nuclear coordinates can be treated separately. As a result of a full decoupling of the total spin and roto-vibrational state of the system, equation (3) becomes

$$\begin{aligned}\left(\frac{\mathrm{d}^2\sigma}{\mathrm{d}\Omega\,\mathrm{d}\omega}\right)^{uncorr} &= \frac{1}{2\pi N}\frac{k_1}{k_0}\int \mathrm{d}t\,\mathrm{e}^{-\mathrm{i}\omega t}\sum_{i,j=1}^{N}\sum_{\nu,\nu'=1}^{n}\sum_{\mu_0} p_{\mu_0}\sum_{S_0} p_{S_0}\langle\mu_0|\langle S_0|\hat{b}^*_{i\nu}\hat{b}_{j\nu'}|S_0\rangle|\mu_0\rangle \\ &\times \sum_{\tau_0} p_{\tau_0}\langle\tau_0|\,\mathrm{e}^{-\mathrm{i}\boldsymbol{Q}\cdot\boldsymbol{R}_i(0)}\,\mathrm{e}^{\mathrm{i}\boldsymbol{Q}\cdot\boldsymbol{R}_j(t)}|\tau_0\rangle\sum_{U_0U_1} p_{U_0}\,\mathrm{e}^{\mathrm{i}\omega_{U_0U_1}t} \\ &\times \langle U_0|\,\mathrm{e}^{-\mathrm{i}\boldsymbol{Q}\cdot\boldsymbol{r}_{i\nu}}|U_1\rangle\langle U_1|\,\mathrm{e}^{\mathrm{i}\boldsymbol{Q}\cdot\boldsymbol{r}_{j\nu'}}|U_0\rangle. \end{aligned} \tag{6}$$

The average over the spin part can be calculated to give $b^{i\nu}_{coh}b^{j\nu'}_{coh} + (b^{i\nu}_{inc})^2\delta_{\nu,\nu'}\delta_{i,j}$. Therefore, by separating into self and distinct contributions, after factorization of the states $|U\rangle$ into single-molecule roto-vibrational $|u\rangle$ states, and by including the intermediate scattering functions, we obtain the equivalent of equation (4) in the uncorrelated case:

$$\begin{aligned}\left(\frac{\mathrm{d}^2\sigma}{\mathrm{d}\Omega\,\mathrm{d}\omega}\right)^{uncorr} &= \frac{1}{2\pi}\frac{k_1}{k_0}\int \mathrm{d}t\,\mathrm{e}^{-\mathrm{i}\omega t}[F_s(Q,t)v(Q,t)^{uncorr} + F_d(Q,t)u(Q)^{uncorr}] \\ &\text{with } v(Q,t)^{uncorr} = \sum_{\nu,\nu'=1}^{n}(b^{\nu}_{coh}b^{\nu'}_{coh} + b^{\nu^2}_{inc}\delta_{\nu,\nu'})\sum_{u_0,u_1} p_{u_0}\mathrm{e}^{\mathrm{i}\omega_{u_0u_1}t} \\ &\times \langle u_0|\,\mathrm{e}^{-\mathrm{i}\boldsymbol{Q}\cdot\boldsymbol{r}_\nu}|u_1\rangle\langle u_1|\,\mathrm{e}^{\mathrm{i}\boldsymbol{Q}\cdot\boldsymbol{r}_{\nu'}}|u_0\rangle \\ &\text{and } u(Q)^{uncorr} = \left|\sum_{\nu=1}^{n} b^{\nu}_{coh}\sum_{u_0} p_{u_0}\langle u_0|\,\mathrm{e}^{\mathrm{i}\boldsymbol{Q}\cdot\boldsymbol{r}_\nu}|u_0\rangle\right|^2 \end{aligned} \tag{7}$$

which will be useful later on.

It is worth pointing out that the model calculations summarized in the following, which take as their main reference and starting point the quantum mechanical treatment of Young and

Koppel for the hydrogens [9] and of Griffing [8] for methane, serve only as a *memento* and basic knowledge for the understanding of subsequent discussion on the effective implementation of these kinds of calculations. To this aim, formulae (originally derived in different papers by different authors) are reported here with uniform notation from one case to another, in order to provide the reader with a single, and hopefully useful, self-consistent 'vade-mecum' in this field.

3. Homonuclear diatomic molecules

3.1. Non-negligible spin correlations

If, as a further hypothesis, intramolecular vibration–rotation coupling is neglected, the stationary states $|w\rangle$ of equation (4) for the internal degrees of freedom of a freely vibro-rotating diatomic molecule are of the form

$$\begin{aligned} &|w\rangle = |JM\rangle|TM_T\rangle|\upsilon\rangle \qquad \text{with} \\ &E_w = [E_{rot} + E_{vib}] = [BJ(J+1) - DJ^2(J+1)^2 + E_{vib}] \\ &p_w = \frac{\exp(-\beta E_w)}{\sum_{w'} \exp(-\beta E_{w'})}, \qquad \beta = (k_B T)^{-1} \end{aligned} \tag{8}$$

where the quantum numbers for rotational, total nuclear spin and vibrational state of the molecule were explicitly introduced, as well as the rotational (D accounts for the centrifugal distortion) and vibrational contributions to the energy of the molecule in state w of probability p_w. However, the required symmetry for the total molecular wavefunction makes possible, in the present case, only those product states $|w\rangle$, where T and J appear with the same parity. Such a restriction applies both for bosons and for fermions. Therefore, as a consequence of the indistinguishability principle, the product states $|w\rangle$ do not form a complete set in either case. According to equation (8) and the above requirements, the corresponding expressions for $v(Q,t)$ and $u(Q)$ in equation (4) become

$$\begin{aligned} v(Q,t) = &\sum_{\mu_0\mu_1} p_{\mu_0} \sum_{J_0T_0}{}^{*} p_{J_0T_0} \sum_{M_0} p_{M_0} \sum_{M_{T_0}} p_{M_{T_0}} \sum_{J_1T_1}{}^{*} \mathrm{e}^{\mathrm{i}\omega_{J_0J_1}t} \sum_{\upsilon_1} \mathrm{e}^{\mathrm{i}\omega_{\upsilon_0\upsilon_1}t} \\ &\times \sum_{M_1} \sum_{M_{T_1}} |\langle\mu_1|\langle J_1M_1|\langle T_1M_{T_1}|\langle\upsilon_1|\hat{O}|\upsilon_0=0\rangle|T_0M_{T_0}\rangle|J_0M_0\rangle|\mu_0\rangle|^2 \end{aligned} \tag{9}$$

$$u(Q) = \sum_{\mu_0\mu_1} p_{\mu_0} \left| \sum_{J_0T_0}{}^{*} p_{J_0T_0} \sum_{M_0} p_{M_0} \sum_{M_{T_0}} p_{M_{T_0}} \langle\mu_1|\langle J_0M_0|\langle T_0M_{T_0}|\langle 0|\hat{O}|0\rangle|T_0M_{T_0}\rangle|J_0M_0\rangle|\mu_0\rangle \right|^2 \tag{10}$$

where the star at the summations over J and T means that these run only on the possible (equal parity) J, T couples. Moreover, molecules were assumed to lie initially in the ground vibrational state ($\upsilon_0 = 0$), which is a more than justified assumption for most systems up to room temperature (the first excited vibrational state lies at 556.76 meV for deuterium, and at 988.43 meV for CD_4, while k_BT at room temperature is about 25 meV).

Before calculating the matrix elements in equations (9) and (10), it is convenient to include explicitly the diatomic and homonuclear nature of the fluid in the expression of the operator $\hat{O}$:

$$\begin{aligned} \hat{O} = \sum_{\nu=1}^{2} \hat{b}_\nu \mathrm{e}^{\mathrm{i}\boldsymbol{Q}\cdot\boldsymbol{r}_\nu} &= \hat{b}_1 \mathrm{e}^{\mathrm{i}\boldsymbol{Q}\cdot\boldsymbol{r}_1} + \hat{b}_2 \mathrm{e}^{\mathrm{i}\boldsymbol{Q}\cdot\boldsymbol{r}_2} = \hat{b}_1 \mathrm{e}^{\mathrm{i}\boldsymbol{Q}\cdot\frac{\boldsymbol{r}}{2}} + \hat{b}_2 \mathrm{e}^{-\mathrm{i}\boldsymbol{Q}\cdot\frac{\boldsymbol{r}}{2}} \\ &= (\hat{b}_1 + \hat{b}_2)\cos\frac{\boldsymbol{Q}\cdot\boldsymbol{r}}{2} + \mathrm{i}(\hat{b}_1 - \hat{b}_2)\sin\frac{\boldsymbol{Q}\cdot\boldsymbol{r}}{2} \end{aligned} \tag{11}$$

with $\boldsymbol{r}$ being the nuclei interdistance vector, at half of which lies the centre of mass of the molecule. The calculation of $v(Q,t)$ implies the evaluation of $|X|^2$, with X given by

$$\begin{aligned} X &= X^{(+)}R^{(+)} + X^{(-)}R^{(-)} \qquad \text{with} \\ R^{(+)} &= \langle J_1 M_1|\langle \upsilon_1| \cos\frac{\boldsymbol{Q}\cdot\boldsymbol{r}}{2}|0\rangle|J_0 M_0\rangle \\ X^{(+)} &= \langle \mu_1|\langle T_1 M_{T_1}|2b_{coh} + \frac{2b_{inc}}{\sqrt{I(I+1)}}(\boldsymbol{s}\cdot\boldsymbol{T})|T_0 M_{T_0}\rangle|\mu_0\rangle \\ R^{(-)} &= \langle J_1 M_1|\langle \upsilon_1| \sin\frac{\boldsymbol{Q}\cdot\boldsymbol{r}}{2}|0\rangle|J_0 M_0\rangle \\ X^{(-)} &= \langle \mu_1|\langle T_1 M_{T_1}|\mathrm{i}\frac{2b_{inc}}{\sqrt{I(I+1)}}\boldsymbol{s}\cdot(\boldsymbol{I}_1 - \boldsymbol{I}_2)|T_0 M_{T_0}\rangle|\mu_0\rangle \end{aligned} \tag{12}$$

where $\boldsymbol{T} = \boldsymbol{I}_1 + \boldsymbol{I}_2$ is the total molecular spin ($I_1 = I_2 = I$). The quantum-mechanical calculation of the matrix elements $R^{(\pm)}$ is performed by assuming harmonic vibrations and taking, since vibration–rotation coupling is neglected and rotations are free, the spherical harmonics as rotational wavefunctions. The direction of the molecule is identified by the polar angles (θ,φ) with respect to the direction of $\boldsymbol{Q}$, so that $\boldsymbol{Q}\cdot\boldsymbol{r} = Qr\eta$ with $\eta = \cos\theta$. Moreover r is expressed as $r = x + R_{eq}$, i.e. as the sum of the equilibrium internuclear distance R_{eq} and the bond stretching x. Use of the quantum algebraic method for the treatment of a linear harmonic oscillator leads to

$$\begin{aligned} R^{(+)} &= \frac{(\mathrm{i}\alpha)^{\upsilon_1}}{2\sqrt{\upsilon_1!}}\langle J_1 M_1|f(\eta)|J_0 M_0\rangle \qquad \text{with } f(\eta) = \mathrm{e}^{-\alpha^2\eta^2/2}\eta^{\upsilon_1}[\mathrm{e}^{\mathrm{i}\beta\eta} + (-1)^{\upsilon_1}\mathrm{e}^{-\mathrm{i}\beta\eta}] \\ R^{(-)} &= \frac{(\mathrm{i}\alpha)^{\upsilon_1}}{2\mathrm{i}\sqrt{\upsilon_1!}}\langle J_1 M_1|\tilde{f}(\eta)|J_0 M_0\rangle \qquad \text{with } \tilde{f}(\eta) = \mathrm{e}^{-\alpha^2\eta^2/2}\eta^{\upsilon_1}[\,\mathrm{e}^{\mathrm{i}\beta\eta} - (-1)^{\upsilon_1}\mathrm{e}^{-\mathrm{i}\beta\eta}] \end{aligned} \tag{13}$$

where $\beta = \frac{1}{2}QR_{eq}$, $\alpha = Q\sqrt{\hbar}/\sqrt{2M\omega_{\mathrm{v}}}$, M is the mass of the molecule and ω_{v} is the frequency of the oscillator such that $E_\upsilon = \hbar\omega_{\mathrm{v}}(\upsilon + \frac{1}{2})$. Note that $f(\eta)$ and $\tilde{f}(\eta)$ are, respectively, an even and an odd function of η, independently of the parity of υ_1. Well-known properties of the spherical harmonics [33, 34] can be used to express the rotational matrix elements in terms of the Clebsch–Gordan (CG) coefficients C and the Legendre polynomials P_l, as ($g(\eta)$ is an even or odd function of η):

$$\begin{aligned} \langle J_1 M_1|g(\eta)|J_0 M_0\rangle &= \frac{(-1)^{M_1}}{2}\sqrt{(2J_1+1)(2J_0+1)}\delta_{M_1,M_0} \\ &\times \sum_{l=|J_1-J_0|}^{J_1+J_0} C(J_1 J_0 l;000)C(J_1 J_0 l;-M_1 M_0 0)\delta_{J_1+J_0+l,2k}\int_{-1}^{1}\mathrm{d}\eta\, g(\eta)P_l(\eta) \end{aligned} \tag{14}$$

which vanishes unless $M_1 = M_0$, $J_1 + J_0 + l$ is even, and $g(\eta)$ has the same parity of l, with $|J_0 - J_1| < l < J_0 + J_1$. Due to these restrictions, and to the parity properties of f and $\tilde{f}$, we find that $R^{(+)} = 0$ if $J_1 + J_0$ is odd (l odd, ΔJ odd) and $R^{(-)} = 0$ if $J_1 + J_0$ is even (l even, ΔJ even). Therefore

$$\sum_{M_0 M_1} p_{M_0}|X|^2 = \begin{cases} |X^{(+)}|^2\displaystyle\sum_{M_0 M_1} p_{M_0}|R^{(+)}|^2 = |X^{(+)}|^2 \\ \quad\times\left[\dfrac{\alpha^{2\upsilon_1}(2J_1+1)}{4\upsilon_1!}\displaystyle\sum_{l\,\text{even}} C^2(J_1 J_0 l;000)|A_{l,\upsilon_1}|^2\right], & \Delta J \text{ even} \\ |X^{(-)}|^2\displaystyle\sum_{M_0 M_1} p_{M_0}|R^{(-)}|^2 = |X^{(-)}|^2 \\ \quad\times\left[\dfrac{\alpha^{2\upsilon_1}(2J_1+1)}{4\upsilon_1!}\displaystyle\sum_{l\,\text{odd}} C^2(J_1 J_0 l;000)|A_{l,\upsilon_1}|^2\right], & \Delta J \text{ odd} \end{cases} \tag{15}$$

where we defined $A_{l,\upsilon_1} = \int_{-1}^{1} \mathrm{d}\eta\, \eta^{\upsilon_1} \mathrm{e}^{-\alpha^2\eta^2/2}\, \mathrm{e}^{\mathrm{i}\beta\eta} P_l(\eta)$ and we used $p_{M_0} = (2J_0+1)^{-1}$. Note, however, that the restriction over the summations in square brackets can be removed, since the CG coefficients are zero in correspondence with the forbidden values of l.

These results, combined with the parity coupling between J and T, the conservation of spin angular momentum ($\Delta T = 0, \pm 1$) and the fact that $X^{(+)} = 0$ if $\Delta T = \pm 1$ and $X^{(-)} = 0$ if $\Delta T = 0$, allows one to evaluate the spin part in $v(Q,t)$ as if summations over T_1 were unrestricted and states $|T_1 M_{T_1}\rangle|\mu_1\rangle$ formed a complete set. For unpolarized neutrons ($p_{\mu_0} = 1/2$), all these considerations lead to

$$\sum_{\mu_0\mu_1} p_{\mu_0} \sum_{T_1 M_{T_1}} |X^{(\pm)}|^2 = \begin{cases} 4b_{coh}^2 + \dfrac{b_{inc}^2}{I(I+1)} T_0(T_0+1), & \Delta J \text{ even} \\ b_{inc}^2 \left[4 - \dfrac{T_0(T_0+1)}{I(I+1)} \right], & \Delta J \text{ odd.} \end{cases} \tag{16}$$

Before deriving the final expression for $v(Q,t)$, one needs to consider how the initial state probabilities $p_{J_0T_0}$ in equation (9) split accordingly with the parity of the rotational levels. By remembering that rotational and spin levels, J and T have, respectively, a $(2J+1)$- and $(2T+1)$-fold degeneracy, the probability $p_{J_0T_0}$ is

$$p_{J_0T_0} = \frac{(2J_0+1)(2T_0+1)\mathrm{e}^{-\beta E_{J_0}}}{\sum^*_{J_0T_0}(2J_0+1)(2T_0+1)\mathrm{e}^{-\beta E_{J_0}}} \tag{17}$$

which correctly takes into account the coupling of J and T. The above probability can be written more conveniently by introducing the even and odd, rotational and spin, partition functions:

$$\begin{aligned} Z_e &= \sum_{J_0 \text{ even}} (2J_0+1)\mathrm{e}^{-\beta E_{J_0}}, & Z_o &= \sum_{J_0 \text{ odd}} (2J_0+1)\mathrm{e}^{-\beta E_{J_0}}, \\ g_e &= \sum_{T_0 \text{ even}} (2T_0+1), & g_o &= \sum_{T_0 \text{ odd}} (2T_0+1), \end{aligned} \tag{18}$$

and evaluating the concentration of the even and odd states ($x_e + x_o = 1$):

$$x_e = \frac{Z_e g_e}{Z_e g_e + Z_o g_o}, \qquad x_o = \frac{Z_o g_o}{Z_e g_e + Z_o g_o}. \tag{19}$$

With these definitions, and by noting that $Z_e g_e + Z_o g_o$ is the denominator at the second member of equation (17), the latter becomes

$$p_{J_0T_0} = \begin{cases} \dfrac{(2J_0+1)(2T_0+1)\mathrm{e}^{-\beta E_{J_0}}}{Z_e g_e} x_e \equiv p^e_{J_0} p^e_{T_0} x_e, & \text{for } J_0 \text{ and } T_0 \text{ even} \\ \dfrac{(2J_0+1)(2T_0+1)\mathrm{e}^{-\beta E_{J_0}}}{Z_o g_o} x_o \equiv p^o_{J_0} p^o_{T_0} x_o, & \text{for } J_0 \text{ and } T_0 \text{ odd} \end{cases} \tag{20}$$

where even and odd, rotational and spin, 'probabilities' were defined as

$$p^{e,o}_{J_0} = \frac{(2J_0+1)\mathrm{e}^{-\beta E_{J_0}}}{Z_{e,o}}, \qquad p^{e,o}_{T_0} = \frac{(2T_0+1)}{g_{e,o}}.$$

The spin partition function can be calculated as a function of the nuclear spin I of the nuclei, and the results are reported in table 1, together with the corresponding values for the species equilibrium concentrations and their so-called *normal* values in the limit of high temperatures, when $Z_e \approx Z_o$.

Thus, different probabilities pertain to the odd and even levels, and the two possible species (even or odd) are identified with the *para* or *ortho* states of the molecule. As summarized in

Table 1. The spin partition function g and species concentrations x as a function of the nuclear spin I of the nuclei for fermions and bosons. The species normal concentration (high temperature limit), x^N, is also reported.

Nuclei kind	J	T	$g_{e,o}$	$x_{e,o}$	$x^N_{e,o}(T\to\infty)$	Species
Fermions	e	e	$I(2I+1)$	$\dfrac{Z_e I}{Z_e I + Z_o(I+1)}$	$\dfrac{I}{2I+1}$	*Para*
	o	o	$(I+1)(2I+1)$	$\dfrac{Z_o(I+1)}{Z_e I + Z_o(I+1)}$	$\dfrac{(I+1)}{2I+1}$	*Ortho*
Bosons	e	e	$(I+1)(2I+1)$	$\dfrac{Z_e(I+1)}{Z_o I + Z_e(I+1)}$	$\dfrac{(I+1)}{2I+1}$	*Ortho*
	o	o	$I(2I+1)$	$\dfrac{Z_o I}{Z_o I + Z_e(I+1)}$	$\dfrac{I}{2I+1}$	*Para*

table 1, for fermions, the *para/ortho* states correspond to *even/odd* rotational levels, and vice versa for bosons (*para/ortho*→*odd/even*). Note also that the para species corresponds to that with the minimum g and with the lowest normal concentration x^N, both for bosons and for fermions.

As a consequence of equations (15), (16) and (20), and by noting that

$$\sum_{J_0T_0}^{*} p_{J_0T_0} \sum_{J_1} \cdots = \begin{cases} \displaystyle\sum_{J_0\,\text{even}} x_e p^{\mathrm{e}}_{J_0} \sum_{T_0\,\text{even}} p^{\mathrm{e}}_{T_0} \sum_{J_1\,\text{even}} \cdots \\ \quad + \displaystyle\sum_{J_0\,\text{odd}} x_o p^{o}_{J_0} \sum_{T_0\,\text{odd}} p^{o}_{T_0} \sum_{J_1\,\text{odd}} \cdots, & \Delta J \text{ even} \\ \displaystyle\sum_{J_0\,\text{even}} x_e p^{e}_{J_0} \sum_{T_0\,\text{even}} p^{e}_{T_0} \sum_{J_1\,\text{odd}} \cdots \\ \quad + \displaystyle\sum_{J_0\,\text{odd}} x_o p^{o}_{J_0} \sum_{T_0\,\text{odd}} p^{o}_{T_0} \sum_{J_1\,\text{even}} \cdots, & \Delta J \text{ odd} \end{cases} \tag{21}$$

we finally arrive at the expression of $v(Q,t)$ allowing for a direct computation:

$$\begin{aligned} v(Q,t) = s_{ee} \sum_{J_0\,\text{even}} x_e p^{e}_{J_0} \sum_{J_1\text{even}} \mathrm{e}^{\mathrm{i}\omega_{J_0J_1}t} \sum_{\upsilon_1} \mathrm{e}^{\mathrm{i}\upsilon_1\omega_\nu t} \frac{\alpha^{2\upsilon_1}}{4\upsilon_1!}(2J_1+1)\sum_{l} C^2(J_1J_0l;000)|A_{l,\upsilon_1}|^2 \\ + s_{oo} \sum_{J_0\,\text{odd}} x_o p^{o}_{J_0} \sum_{J_1\,\text{odd}} \cdots + s_{eo} \sum_{J_0\,\text{even}} x_e p^{e}_{J_0} \sum_{J_1\,\text{odd}} \cdots \\ + s_{oe} \sum_{J_0\,\text{odd}} x_o p^{o}_{J_0} \sum_{J_1\,\text{even}} \cdots \end{aligned} \tag{22}$$

where the coefficients s are those defined and calculated in table 2. Note that the similar expression derived in [19] in terms of $3j$ symbols (equation (3.4) there) suffers from two misprints: the exponent 2 at α is missing, as well as a factor $1/\hbar$ in the exponential function.

The specific s coefficients for H_2 and D_2 can be derived by using the values $I = 1/2$ and 1, respectively, in the expressions of table 2. A peculiarity of H_2 is that transitions between *even* levels are weighted exclusively by b^2_{coh}, while those involving a change of parity are weighted by b^2_{inc} only.

Equation (22) can also be rewritten in a more compact form, which is particularly suited to computer programming, as

$$v(Q,t) = \sum_{J_0J_1\upsilon_1 l} \mathrm{e}^{\mathrm{i}\omega_{J_0J_1}t}\,\mathrm{e}^{\mathrm{i}\upsilon_1\omega_\nu t} F(Q, J_0, J_1, \upsilon_1, l) \tag{23}$$

Table 2. The s coefficients of equation (22), according to the calculations outlined in equations (9), (16) and (20). Expressions as a function of the nuclear spin I are shown both for fermions and bosons.

s	Fermions (I half-integer)	Bosons (I integer)
$s_{ee} = \sum_{T_0\ even} p^e_{T_0}\left[4b^2_{coh} + \frac{b^2_{inc}}{I(I+1)}T_0(T_0+1)\right]$	$4b^2_{coh} + b^2_{inc}\frac{(2I-1)}{I}$	$4b^2_{coh} + b^2_{inc}\frac{(2I+3)}{I+1}$
$s_{eo} = \sum_{T_0\ even} p^e_{T_0} b^2_{inc}\left[4 - \frac{T_0(T_0+1)}{I(I+1)}\right]$	$b^2_{inc}\frac{(2I+1)}{I}$	$b^2_{inc}\frac{(2I+1)}{I+1}$
$s_{oe} = \sum_{T_0\ odd} p^o_{T_0} b^2_{inc}\left[4 - \frac{T_0(T_0+1)}{I(I+1)}\right]$	$b^2_{inc}\frac{(2I+1)}{I+1}$	$b^2_{inc}\frac{(2I+1)}{I}$
$s_{oo} = \sum_{T_0\ odd} p^o_{T_0}\left[4b^2_{coh} + \frac{b^2_{inc}}{I(I+1)}T_0(T_0+1)\right]$	$4b^2_{coh} + b^2_{inc}\frac{(2I+3)}{I+1}$	$4b^2_{coh} + b^2_{inc}\frac{(2I-1)}{I}$

where

$$F(Q, J_0, J_1, \upsilon_1, l) = s_{(J_0J_1)}x_{(J_0)}p^{(J_0)}_{J_0}\frac{\alpha^{2\upsilon_1}}{4\upsilon_1!}(2J_1+1)\sum_l C^2(J_1J_0l;000)|A_{l,\upsilon_1}|^2, \tag{24}$$

and the subscripts and superscripts in brackets mean that the quantities vary, according to the previous definitions of tables 1 and 2, with the parity of J_0, or of J_0 and J_1.

Equation (22) (or (23)) is the generalization to harmonically vibrating molecules of the rigid rotating molecule analogue discussed by Sears [13]. In principle, no further approximations are required nowadays to carry out the calculation, since the A_{l,υ_1}'s can be computed, to a good accuracy, by numerical integration and no expansion of the above integrals (as was done in [19] for the case $\upsilon_1 = 0$) is apparently necessary. It is worth noting, however, that great care must be taken if high values of l are involved, since the integrands become more and more rapidly oscillating functions of η with increasing l and with approaching the upper bound $\eta = 1$. Therefore their integration must be duly checked. Fortunately, the calculation of the A_{l,υ_1}'s at high l values ($l > 20$) is rarely needed, since this implies the combination of a rather high incident neutron energy and a high (>300 K) temperature of the sample (i.e. many Stokes and anti-Stokes transitions are allowed), which is usually not the case in most applications. At any rate, if high l values can occur, the product $C^2(J_1J_0l;000)|A_{l,\upsilon_1}|^2$ can be verified to be an increasingly negligible fraction of the dominant, small l, terms. In addition, initial state probabilities further kill out such contributions and final results will not suffer if the computation is performed by limiting the summations over l below a reasonable (checked) value. Better examples related to this problem will be given in the following, for the case of chlorine, since high l values can occur not only because of the temperature and neutron energy, but mainly when rotational levels are narrowly spaced, as happens for the heavier diatomic molecules.

To complete the basics of the diatomic case in the presence of spin correlations, we now turn to $u(Q)$. Due to the identity of the initial and final molecular states in equation (10), the previously discussed selection rule ($R^{(-)} = 0$ for ΔJ even) leads in this case to the calculation of $X^{(+)}_0 R^{(+)}_0$, with

$$\begin{aligned} R^{(+)}_0 &= \tfrac{1}{2}\langle J_0M_0|f(\eta, \upsilon_1 = 0)|J_0M_0\rangle \\ X^{(+)}_0 &= \langle\mu_1|\langle T_0M_{T_0}|2b_{coh} + \frac{2b_{inc}}{\sqrt{I(I+1)}}(\boldsymbol{s}\cdot\boldsymbol{T})|T_0M_{T_0}\rangle|\mu_0\rangle. \end{aligned} \tag{25}$$

The first of the above equations is obtained from equation (13) with $\upsilon_1 = 0$. Use of equation (14) with $J_1 = J_0$ and of the properties [34]

$$\sum_{M_0} p_{M_0}(-1)^{M_0} C(J_0 J_0 l; -M_0 M_0 0) = (-1)^{J_0} \frac{\delta_{l0}}{\sqrt{2J_0+1}} \text{ and } C(J_0 J_0 0; 000) = \frac{(-1)^{J_0}}{\sqrt{2J_0+1}},$$

provide

$$\sum_{M_0} p_{M_0} R_0^{(+)} = \frac{A_{00}}{2}. \tag{26}$$

Concerning the spin part, through the use of raising and lowering operators for $\boldsymbol{s}$ and $\boldsymbol{T}$, it is easily found that $X_0^{(+)} = 2b_{coh}\delta_{\mu_1,\mu_0}$, and thus equation (10) reduces to

$$u(Q) = \sum_{\mu_0} p_{\mu_0} \sum_{\mu_1} \left| \sum_{J_0 T_0}{}^{*} p_{J_0 T_0} \frac{A_{00}}{2} 2b_{coh}\delta_{\mu_0\mu_1} \right|^2 = b_{coh}^2 |A_{00}|^2. \tag{27}$$

3.2. Negligible spin correlations

By performing the summation over the nuclei in the diatomic case (υ, $\upsilon' = 1, 2$) and introducing the internuclear distance vector $\boldsymbol{r}$, then $v(Q,t)$ and $u(Q)$ in equation (7) become

$$\begin{aligned} v(Q,t)^{uncorr} &= \sum_{u_0,u_1} p_{u_0} \, \mathrm{e}^{\mathrm{i}\omega_{u_0u_1}t} \Bigg[b_{coh}^2 |\langle u_1| 2\cos\frac{\boldsymbol{Q}\cdot\boldsymbol{r}}{2} |u_0\rangle|^2 \\ &\quad + b_{inc}^2 \left(|\langle u_1| \, \mathrm{e}^{\mathrm{i}\boldsymbol{Q}\cdot\boldsymbol{r}/2} |u_0\rangle|^2 + |\langle u_1| \mathrm{e}^{-\mathrm{i}(\boldsymbol{Q}\cdot\boldsymbol{r})/2} |u_0\rangle|^2 \right) \Bigg] \\ u(Q)^{uncorr} &= 4b_{coh}^2 \left| \sum_{u_0} p_{u_0} \langle u_0| \cos\frac{\boldsymbol{Q}\cdot\boldsymbol{r}}{2} |u_0\rangle \right|^2. \end{aligned} \tag{28}$$

As was done in the previous subsection, a quantum mechanical treatment of rotations and harmonic vibrations leads to

$$\begin{aligned} v(Q,t)^{uncorr} &= \sum_{J_0 J_1 \upsilon_1} p_{J_0} \, \mathrm{e}^{\mathrm{i}\omega_{J_0J_1}t} \, \mathrm{e}^{\mathrm{i}\upsilon_1\omega_\upsilon t} \Bigg[4b_{coh}^2 \sum_{M_0 M_1} p_{M_0} |R^{(+)}|^2 \\ &\quad + b_{inc}^2 \frac{\alpha^{2\upsilon_1}(2J_1+1)}{2\upsilon_1!} \sum_l C^2(J_1 J_0 l; 000) |A_{l,\upsilon_1}|^2 \Bigg] \\ u(Q)^{uncorr} &= 4b_{coh}^2 \left| \sum_{J_0 M_0} p_{J_0} p_{M_0} R_0^{(+)} \right|^2 \end{aligned} \tag{29}$$

where definitions given in equations (12)–(15) and (25) were used, and we assumed $|u\rangle = |JM\rangle|\upsilon\rangle$. Exploiting the first of equations (15), the square bracket in equation (29) turns out to be

$$\frac{\alpha^{2\upsilon_1}(2J_1+1)}{4\upsilon_1!} \left[(4b_{coh}^2 + 2b_{inc}^2) \sum_{l\,\mathrm{even}} C^2(J_1 J_0 l; 000) |A_{l,\upsilon_1}|^2 + 2b_{inc}^2 \sum_{l\,\mathrm{odd}} C^2(J_1 J_0 l; 000) |A_{l,\upsilon_1}|^2 \right]. \tag{30}$$

Finally, by using a more compact form of equation (30), and remembering equations (23) and (26), it is found that

$$v(Q,t)^{uncorr} = \sum_{J_0 J_1 \upsilon_1 l} \mathrm{e}^{\mathrm{i}\omega_{J_0 J_1} t}\, \mathrm{e}^{\mathrm{i}\upsilon_1 \omega_\nu t} F(Q, J_0, J_1, \upsilon_1, l)^{uncorr}, \qquad u(Q)^{uncorr} = b_{coh}^2 |A_{00}|^2$$

with

$$F(Q, J_0, J_1, \upsilon_1, l)^{uncorr} = p_{J_0} \frac{\alpha^{2\upsilon_1}(2J_1+1)}{4\upsilon_1!} 2[b_{coh}^2 + b_{inc}^2 + (-1)^l b_{coh}^2] \times C^2(J_1 J_0 l; 000)|A_{l,\upsilon_1}|^2. \tag{31}$$

Thus, also in the present uncorrelated case, we derived rather general expressions for the inter- and intramolecular cross-sections of a diatomic molecule, which represent an improvement with respect to what is available in the literature. For instance, the intramolecular cross-section calculated in equation (23) of [18] corresponds only to the rigid molecule case, though modified through a Debye–Waller factor in order to account at least for zero-point vibrations. Here no such limitations are present, and appropriate tools for the calculation in the presence of vibrational transitions ($\upsilon_1 \neq 0$) are given. However, in most applications of the above formulae (equations (23) and (31)) related to reactor-based experiments, the incident thermal—or even hot (>160 meV)—neutron energy will rarely be enough to excite vibrational transitions and, quite often, only zero-point motion needs to be retained, by limiting the calculations to the $\upsilon_1 = 0$ case. This does not hold in connection with pulsed source time-of-flight diffraction measurements, where such models, due to the wide range of energies (up to a few electron volts) composing the incident polychromatic beam, turn out to be inapplicable.

4. Spherical-top molecules: uncorrelated-spin case

We now consider the calculation of the inter- and intramolecular cross-sections, $u(Q)$ and $v(Q,t)$, for spherical top molecules of the kind YX_4, with negligible spin correlations. Starting from equation (7), and assuming negligible rotation–vibration coupling, we once again adopt the factorization $|u\rangle = |JMK\rangle|\upsilon\rangle$ into rotational and vibrational eigenstates, to write

$$\begin{aligned} v(Q,t)^{uncorr} &= \sum_{\nu,\nu'} a_{\nu\nu'} \sum_{J_0, M_0, K_0, \upsilon_0} p_{J_0} p_{M_0} p_{K_0} p_{\upsilon_0} \sum_{J_1, M_1, K_1, \upsilon_1} \mathrm{e}^{\mathrm{i}\omega_{J_0 J_1} t} \\ &\quad \times \langle J_1 M_1 K_1 |\, \mathrm{e}^{\mathrm{i}\boldsymbol{Q}\cdot\boldsymbol{R}_{\nu'}^{eq}} \langle \upsilon_1 |\, \mathrm{e}^{\mathrm{i}\boldsymbol{Q}\cdot\boldsymbol{x}_{\nu'}(t)} |\upsilon_0\rangle |J_0 M_0 K_0\rangle \\ &\quad \times \langle J_0 M_0 K_0 | \mathrm{e}^{-\mathrm{i}\boldsymbol{Q}\cdot\boldsymbol{R}_{\nu}^{eq}} \langle \upsilon_0 | \mathrm{e}^{-\mathrm{i}\boldsymbol{Q}\cdot\boldsymbol{x}_{\nu}} |\upsilon_1\rangle |J_1 M_1 K_1\rangle \\ u(Q)^{uncorr} &= \left| \sum_{\nu=1}^{n} b_{coh}^{\nu} \sum_{J_0, M_0, K_0, \upsilon_0} p_{J_0} p_{M_0} p_{K_0} p_{\upsilon_0} \langle J_0 M_0 K_0 |\, \mathrm{e}^{\mathrm{i}\boldsymbol{Q}\cdot\boldsymbol{R}_{\nu}^{eq}} \langle \upsilon_0 |\, \mathrm{e}^{\mathrm{i}\boldsymbol{Q}\cdot\boldsymbol{x}_{\nu}} |\upsilon_0\rangle |J_0 M_0 K_0\rangle \right|^2 \end{aligned} \tag{32}$$

where $a_{\nu\nu'} = b_{coh}^{\nu} b_{coh}^{\nu'} + (b_{inc}^{\nu})^2 \delta_{\nu,\nu'}$, $\boldsymbol{r}_\nu$ was expressed as the sum of the equilibrium position vector with respect to the CM and the displacement vector from equilibrium due to vibrations ($\boldsymbol{r}_\nu = \boldsymbol{R}_\nu^{eq} + \boldsymbol{x}_\nu$), and, finally, the proper rotational structure of a spherical-top molecule, degenerate both with respect to a direction (z) in fixed space (individuated by M, as usual) and to a fixed direction (ζ) in the molecule reference frame (individuated by the quantum number K), was taken into account [17, 32]. It is worth remembering, in this last respect, that the rotational eigenfunctions of a spherical-top molecule are of the form (where $\Omega = (\alpha, \beta, \gamma)$ are the Euler angles and D's are the rotation matrices [17])

$$|JMK\rangle = \sqrt{\frac{2J+1}{8\pi^2}} D_{MK}^{(J)}(\Omega),$$

and that the operators $\boldsymbol{J}^2$, J_z and J_ζ commute, with eigenvalues over the $|JMK\rangle$ states given by $J(J+1)$, M and K, respectively. Consequently, a given rotational level J, whose energy

takes the usual form in terms of the rotational constant B, has a $(2J+1)^2$-fold degeneracy, if spin correlations are neglected [32].

Note that, for convenience of subsequent treatment, the time-dependent Heisenberg representation of the operator $\boldsymbol{x}_{\nu'}$ has been re-introduced in the first of equations (32). Moreover, the vibrational states of the molecule, still globally indicated as $|\upsilon\rangle$ in equation (32), must now be thought of as characterized by the various occupation numbers corresponding to the λ normal modes of vibration of the molecule, i.e. $|\upsilon\rangle = |n_1 \cdots n_\lambda\rangle$, where $\lambda = 9$ for YX_4 molecules [4]. As before, the ground vibrational state is assumed as initial condition ($n_\lambda = 0$ for each λ, initially).

Previous treatments of the—thermal and orientation—average of the vibrational part in the computation of the double-differential cross-section of spherical-top molecules often refer to the (quite common) case in which neutrons are unable to excite vibrational transitions [5, 6, 8, 11, 15–17]. In this picture, matrix elements involve only zero-point vibrations, and their average can be effectively represented by Debye–Waller factors. The latter were calculated by Pope for YX_4 molecules [4], although never employed in their complete version in all subsequent papers on methane (including [26]). Despite the difficulties related to the interpretation of such a complex (and unavoidably misprint-abundant) paper [4], we shall try to comment and make use, in the following, of the complete set of Debye–Waller factors provided by Pope for YX_4 molecules. This is done in the attempt of improving, for instance, the level of accuracy of nowadays possible CH_4/CD_4 calculations in the case of zero-point vibrations, also providing the reader with verified and user-friendly coefficients.

However, a step forward can be proposed in order to account, at least, for vibrational transitions involving the single (i.e. with a final occupation number equal to 1) excitation of one mode. In other words, processes known as 'one-phonon scattering' in neutron spectroscopy on solids can be treated quite smoothly in the case of a fluid composed of spherical tops, when 'one-phonon' vibrational transitions of the kind $|\upsilon_0\rangle = |00\ldots00\ldots0\rangle \rightarrow |\upsilon_1\rangle = |00\ldots10\ldots0\rangle$ are considered, and the incident energy is anyway not enough to excite more than one mode. In complete analogy with the case of solids, the displacement vector $\boldsymbol{x}_{\nu'}(t)$ can be expressed as the superposition of the normal modes of the molecule according to

$$\boldsymbol{x}_{\nu'}(t) = \sum_\lambda \sqrt{\frac{\hbar}{2m_{\nu'}\omega_\lambda}}[\boldsymbol{e}_{\nu'\lambda}\mathrm{e}^{-\mathrm{i}\omega_\lambda t}a_\lambda + \boldsymbol{e}^*_{\nu'\lambda}\,\mathrm{e}^{\mathrm{i}\omega_\lambda t}a^+_\lambda] \tag{33}$$

where ω_λ is the frequency of the λth mode and $\boldsymbol{e}_{\nu'\lambda}$ is the eigenvector of this mode for nucleus ν' of mass $m_{\nu'}$. The operators a_λ and a^+_λ destroy and create, respectively, a quantum of harmonic oscillator in the λth mode. By using equation (33), together with the well-known properties of a_λ and a^+_λ, and the relation $\mathrm{e}^A\mathrm{e}^B = \mathrm{e}^{A+B+1/2[A,B]}$ for the exponential of operators, the generic vibrational matrix element can be written as

$$\begin{aligned}\langle\upsilon_1|\,\mathrm{e}^{\mathrm{i}\boldsymbol{Q}\cdot\boldsymbol{x}_{\nu'}(t)}|0\rangle &= \langle n_{1,1}\cdots n_{\lambda,1}|\prod_\lambda \exp[\mathrm{i}\alpha_{\nu'\lambda}\boldsymbol{Q}\cdot(\boldsymbol{e}_{\nu'\lambda}\mathrm{e}^{-\mathrm{i}\omega_\lambda t}a_\lambda + \boldsymbol{e}^*_{\nu'\lambda}\,\mathrm{e}^{\mathrm{i}\omega_\lambda t}a^+_\lambda)]|0\ldots0\rangle \\ &= \exp\left(\mathrm{i}\sum_\lambda n_{\lambda,1}\omega_\lambda t\right)\prod_\lambda \exp(-\beta_{\nu'\lambda})\frac{(\mathrm{i}\alpha_{\nu'\lambda}\boldsymbol{Q}\cdot\boldsymbol{e}^*_{\nu'\lambda})^{n_{\lambda,1}}}{\sqrt{n_{\lambda,1}!}}\end{aligned} \tag{34}$$

where the Taylor expansion was also used for the exponentials and we defined

$$\begin{aligned}\alpha_{\nu'\lambda} &= \sqrt{\frac{\hbar}{2m_{\nu'}\omega_\lambda}} \\ \beta_{\nu'\lambda} &= \frac{\alpha^2_{\nu'\lambda}}{2}|\boldsymbol{Q}\cdot\boldsymbol{e}_{\nu'\lambda}|^2.\end{aligned} \tag{35}$$

A reasonable estimate of $v(Q,t)$ can then be derived by separating the orientation average of the time-independent vibrational matrix elements, i.e. $\langle\langle \upsilon_1|\, \mathrm{e}^{\mathrm{i}\boldsymbol{Q}\cdot\boldsymbol{x}_{\nu'}}|0\rangle\langle 0|\mathrm{e}^{-\mathrm{i}\boldsymbol{Q}\cdot\boldsymbol{x}_{\nu}}|\upsilon_1\rangle\rangle_\Omega$, from the rotational part in equation (32) (the time dependence depicted in equation (34) will not be forgotten in the following). In order to simplify things, evaluation of the above average, defined here as $\langle z_{\nu\nu'}\rangle$, can be limited to elastic (all $n_{\lambda,1}=0$) and lowest-order 'one-phonon' (only one $n_{\lambda,1}=1$) scattering only. By means of equation (34), it is found in this case that

$$\langle z_{\nu\nu'}\rangle = \begin{cases} \displaystyle\prod_\lambda \mathrm{e}^{\langle -\beta_{\nu'\lambda}-\beta_{\nu\lambda}\rangle}, & \text{if } n_\lambda = 0 \\ \displaystyle\prod_\lambda \mathrm{e}^{\langle -\beta_{\nu'\lambda}-\beta_{\nu\lambda}\rangle}(\alpha_{\nu'\lambda}\alpha_{\nu\lambda})\frac{\boldsymbol{e}_{\nu'\lambda}\cdot\boldsymbol{e}_{\nu\lambda}}{3}Q^2, & \text{if } n_\lambda = 1. \end{cases} \tag{36}$$

Commonly used approximations are hidden in the result of equation (36): the average of a product was taken as a product of averages, and the average of exponentials were taken as exponentials of averages. The elastic scattering case (zero-point motions only) in equation (36) can be recognized to lead to the well-known definition of Debye–Waller coefficients $\gamma_{\nu\nu'}$ [17]:

$$\prod_\lambda \mathrm{e}^{\langle -\beta_{\nu'\lambda}-\beta_{\nu\lambda}\rangle} = \exp\left[-\sum_\lambda \frac{\hbar Q^2}{12\omega_\lambda}\left(\frac{e_{\nu\lambda}^2}{m_\nu}+\frac{e_{\nu'\lambda}^2}{m_{\nu'}}\right)\right] = \exp(-Q^2\gamma_{\nu\nu'}), \tag{37}$$

while the second of equations (36) gives a tool for double neutron cross-section calculations when one mode can be excited to lowest order.

Carrying out the summation over nuclei in equation (32), and remembering that there are four equal nuclei of type X and one nucleus Y (whose equilibrium position coincides with the CM of the molecule) it is found that $v(Q,t)$ can be written as

$$\begin{aligned} v(Q,t)^{uncorr} = {} & \sum_{\{n_{\lambda,1}\}}\sum_{J_0,J_1} p_{J_0}\exp(\mathrm{i}\omega_{J_0J_1}t)\exp\left(\mathrm{i}\sum_\lambda n_{\lambda,1}\omega_\lambda t\right) \\ & \times\left[a_{XX}\chi_{XX}\sum_{i=1}^4\langle z_{X_iX_i}\rangle + a_{XX'}\chi_{XX'}\sum_{\substack{i,j=1\\ i\neq j}}^4\langle z_{X_iX_j}\rangle\right. \\ & \left. + 2a_{YX}\chi_{YX}\sum_{i=1}^4\langle z_{YX_i}\rangle + a_{YY}\chi_{YY}\langle z_{YY}\rangle\right] \end{aligned} \tag{38}$$

which, in the case of zero-point vibrations only, reduces to

$$\begin{aligned} v(Q,t)^{uncorr} = {} & \sum_{J_0,J_1} p_{J_0}\,\mathrm{e}^{\mathrm{i}\omega_{J_0J_1}t}(4a_{XX}\mathrm{e}^{-Q^2\gamma_{XX}}\chi_{XX} + 12a_{XX'}\mathrm{e}^{-Q^2\gamma_{XX'}}\chi_{XX'} \\ & + 8a_{YX}\mathrm{e}^{-Q^2\gamma_{YX}}\chi_{YX} + a_{YY}\mathrm{e}^{-Q^2\gamma_{YY}}\chi_{YY}) \end{aligned} \tag{39}$$

where

$$\begin{aligned} a_{XX} &= b_{coh\,X}^2 + b_{inc\,X}^2 \\ a_{YX} &= b_{coh\,Y}b_{coh\,X} \\ a_{XX'} &= b_{coh\,X}^2 \\ a_{YY} &= b_{coh\,Y}^2 + b_{inc\,Y}^2 \end{aligned} \tag{40}$$

and

$$\begin{aligned}
\chi_{XX} &= \sum_{M_0,M_1} p_{M_0} \sum_{K_0,K_1} p_{K_0} |\langle J_1 M_1 K_1| \, \mathrm{e}^{\mathrm{i}\boldsymbol{Q}\cdot\boldsymbol{R}_X^{eq}} |J_0 M_0 K_0\rangle|^2 \\
\chi_{YX} &= \sum_{M_0,M_1} p_{M_0} \sum_{K_0,K_1} p_{K_0} \langle J_0 M_0 K_0| \mathrm{e}^{-\mathrm{i}\boldsymbol{Q}\cdot\boldsymbol{R}_Y^{eq}} |J_1 M_1 K_1\rangle \langle J_1 M_1 K_1| \, \mathrm{e}^{\mathrm{i}\boldsymbol{Q}\cdot\boldsymbol{R}_X^{eq}} |J_0 M_0 K_0\rangle \\
\chi_{XX'} &= \sum_{M_0,M_1} p_{M_0} \sum_{K_0,K_1} p_{K_0} \langle J_0 M_0 K_0| \mathrm{e}^{-\mathrm{i}\boldsymbol{Q}\cdot\boldsymbol{R}_X^{eq}} |J_1 M_1 K_1\rangle \langle J_1 M_1 K_1| \, \mathrm{e}^{\mathrm{i}\boldsymbol{Q}\cdot\boldsymbol{R}_{X'}^{eq}} |J_0 M_0 K_0\rangle \\
\chi_{YY} &= \sum_{M_0,M_1} p_{M_0} \sum_{K_0,K_1} p_{K_0} |\langle J_1 M_1 K_1| \, \mathrm{e}^{\mathrm{i}\boldsymbol{Q}\cdot\boldsymbol{R}_Y^{eq}} |J_0 M_0 K_0\rangle|^2 .
\end{aligned} \tag{41}$$

To proceed with the calculation one needs to evaluate the generic rotational matrix element given by

$$\langle J_1 M_1 K_1| \mathrm{e}^{\mathrm{i}\boldsymbol{Q}\cdot\boldsymbol{R}_\nu^{eq}} |J_0 M_0 K_0\rangle = \int \mathrm{d}\Omega \, \frac{\sqrt{(2J_1+1)(2J_0+1)}}{8\pi^2} D^{(J_1)*}_{M_1 K_1} \mathrm{e}^{\mathrm{i}\boldsymbol{Q}\cdot\boldsymbol{R}_\nu^{eq}} D^{(J_0)}_{M_0 K_0} \tag{42}$$

where, using the results of [33, appendices B and C], it can be shown that

$$\mathrm{e}^{\mathrm{i}\boldsymbol{Q}\cdot\boldsymbol{R}_\nu^{eq}} = 4\pi \sum_{l=0}^{\infty} \sum_{n=-l}^{l} \mathrm{i}^l \, j_l(QR_\nu^{eq}) Y_l^{n*}(\Theta_\nu, \Phi_\nu) \sum_{n'=-l}^{l} Y_l^{n'}(\theta_Q, \varphi_Q) D^l_{n'n}(\alpha, \beta, \gamma). \tag{43}$$

In equation (43), the spherical Bessel functions j_l were introduced, as well as the spherical harmonics Y_l^n. The angular coordinates of $\boldsymbol{R}_\nu^{eq}$ and $\boldsymbol{Q}$—marked by the subscript ν and Q, respectively—are (θ, φ) in fixed space and (Θ, Φ) in the molecule reference frame. By using (43), equation (42) becomes

$$\begin{aligned}
\langle J_1 M_1 K_1| \, \mathrm{e}^{\mathrm{i}\boldsymbol{Q}\cdot\boldsymbol{R}_\nu^{eq}} |J_0 M_0 K_0\rangle &= \frac{\sqrt{(2J_1+1)(2J_0+1)}}{2\pi} \\
&\times \sum_{l=0}^{\infty} \sum_{n,n'=-l}^{l} \mathrm{i}^l \, j_l(QR_\nu^{eq}) Y_l^{n*}(\Theta_\nu, \Phi_\nu) Y_l^{n'}(\theta_Q, \varphi_Q) \int \mathrm{d}\Omega \, D^{(J_1)*}_{M_1 K_1} D^l_{n'n} D^{(J_0)}_{M_0 K_0}.
\end{aligned} \tag{44}$$

Various known results [33, 34, appendices] can be used to manipulate the integral in equation (44), which, in terms of the $3j$ symbols, turns out to be

$$\int \mathrm{d}\Omega \, D^{(J_1)*}_{M_1 K_1} D^l_{n'n} D^{(J_0)}_{M_0 K_0} = 8\pi^2 (-1)^{M_1 - K_1} \begin{pmatrix} J_0 & J_1 & l \\ M_0 & -M_1 & n' \end{pmatrix} \begin{pmatrix} J_0 & J_1 & l \\ K_0 & -K_1 & n \end{pmatrix}. \tag{45}$$

The expressions in equation (41), can then be evaluated using equations (42)–(45) and the orthogonality relations [33]:

$$\begin{aligned}
&\sum_{M_0 M_1} \begin{pmatrix} J_0 & J_1 & l \\ M_0 & -M_1 & n' \end{pmatrix} \begin{pmatrix} J_0 & J_1 & l_1 \\ M_0 & -M_1 & n'_1 \end{pmatrix} = \frac{\Delta(J_0 J_1 l)}{2l+1} \delta_{ll_1} \delta_{n'n'_1} \\
&\sum_{K_0 K_1} \begin{pmatrix} J_0 & J_1 & l \\ K_0 & -K_1 & n \end{pmatrix} \begin{pmatrix} J_0 & J_1 & l_1 \\ K_0 & -K_1 & n_1 \end{pmatrix} = \frac{\Delta(J_0 J_1 l)}{2l+1} \delta_{ll_1} \delta_{nn_1} \\
&\Delta(J_0 J_1 l) = 1 \qquad \text{if } |J_0 - J_1| < l < J_0 + J_1; \qquad 0 \text{ otherwise.}
\end{aligned} \tag{46}$$

Doing so, and remembering that $p_{M_0}p_{K_0} = (2J_0+1)^{-2}$, we derive

$$\begin{aligned}
\chi_{XX} &= \frac{2J_1+1}{2J_0+1}\sum_{l=|J_0-J_1|}^{J_0+J_1} j_l^2(QR_X^{eq}) \\
\chi_{YX} &= \frac{2J_1+1}{2J_0+1} j_0(QR_X^{eq})\delta_{J_0,J_1} \\
\chi_{XX'} &= \frac{2J_1+1}{2J_0+1}\sum_{l=|J_0-J_1|}^{J_0+J_1} j_l^2(QR_X^{eq}) P_l(\cos\psi_{XX'}) \\
\chi_{YY} &= \frac{2J_1+1}{2J_0+1}\delta_{J_0,J_1}.
\end{aligned} \tag{47}$$

The symmetry of the molecule allows one to know $\psi_{XX'}$, i.e. the angle between $\boldsymbol{R}_X^{eq}$ and $\boldsymbol{R}_{X'}^{eq}$. In particular, by simple geometrical considerations, it results in $\cos\psi_{XX'} = -1/3$.

For comparison with other papers, it is useful to rewrite the self part of the double-differential cross-section (equation (7)). In this case, it is

$$\begin{aligned}
\frac{k_0}{k_1}\left(\frac{\mathrm{d}^2\sigma}{\mathrm{d}\Omega\,\mathrm{d}\omega}\right)_s^{uncorr} &= \sum_{\{n_{\lambda,1}\}}\sum_{J_0J_1} p_{J_0} S_s\left(Q, \omega - \omega_{J_0J_1} - \sum_\lambda n_{\lambda,1}\omega_\lambda\right)\frac{2J_1+1}{2J_0+1} \\
&\times \left\{\left[a_{YY}\langle z_{YY}\rangle + 2a_{YX}\sum_{i=1}^{4}\langle z_{YX_i}\rangle j_0(QR_X^{eq})\right]\delta_{J_0J_1}\right. \\
&+ \left.\sum_l j_l^2(QR_X^{eq})\left[a_{XX}\sum_{i=1}^{4}\langle z_{X_iX_i}\rangle + a_{XX'}\sum_{\substack{i,j=1\\ i\neq j}}^{4}\langle z_{X_iX_j}\rangle P_l(-\tfrac{1}{3})\right]\right\}
\end{aligned} \tag{48}$$

where equations (5), (38) and (47) were used. In equation (48), the first summation symbol runs over the possible sets of occupation numbers $\{n_{\lambda,1}\}$ compatible with the incident energy and with the hypothesis made before equation (36).

Note that, by comparison with equations (11)–(16) of [8], here a factor 2 does not result in the rotational part of both the XX' term and the YX term. The same was found and applied [35] in the calculations of [26]. Moreover, apart from the generalization proposed here for the Debye–Waller factors, the XX' term reported in equation (48) is the general and quite simple expression substituting the rather misleading and unnecessarily approximate one of [8] (after equation (13), there), still used in recent calculations [26, 35].

We finally remember that the probability p_{J_0} for a spherical top molecule is [32]

$$p_{J_0} = \frac{\mathrm{e}^{-\beta E_{J_0}}(2J_0+1)^2}{\sum_{J_0}\mathrm{e}^{-\beta E_{J_0}}(2J_0+1)^2} \tag{49}$$

which represents the probability of a given rotational level (J), independent of the values of M and K. The above expression should thus be used in equations (38), (39) or (48), in order to correctly perform the calculations. Differently, Marshall and Lovesey [p 458 and ff] [17] report and use, on the whole, another formula. Even by carefully taking into account the various differences related to the adopted notation, we always find a mismatching result, leading us to think of a misprint in the above [17] concerning equation 12.78 there.

Turning to the calculation of the distinct term, $u(Q)$, it is convenient to write the square modulus in equation (32) as

$$u(Q)^{uncorr} = \sum_{\nu,\nu'=1}^{n} b_{coh}^{\nu} b_{coh}^{\nu'} A(\nu)B(\nu') \tag{50}$$

with

$$A(\nu)B(\nu') = \mathrm{e}^{-\gamma_{\nu\nu'}Q^2} \sum_{J_0 M_0 K_0} p_{J_0} p_{M_0} p_{K_0} \langle J_0 M_0 K_0 | \, \mathrm{e}^{\mathrm{i}\boldsymbol{Q}\cdot\boldsymbol{R}_\nu^{eq}} | J_0 M_0 K_0 \rangle \times \sum_{J_0' M_0' K_0'} p_{J_0'} p_{M_0'} p_{K_0'} \langle J_0' M_0' K_0' | \mathrm{e}^{-\mathrm{i}\boldsymbol{Q}\cdot\boldsymbol{R}_{\nu'}^{eq}} | J_0' M_0' K_0' \rangle \tag{51}$$

where the only admitted initial and final vibrational levels ($\upsilon_0 = \upsilon_1 = 0$) for the calculation of $u(Q)$ were explicitly considered, and consequently only the first of equations (36) was used for the average of the vibrational part. By adopting the notation of equation (37) for the Debye–Waller factors in this special case, and by noting that equation (42) reduces to $j_0(QR_\nu^{eq})$ when the initial and final states coincide, equation (50) becomes

$$u(Q) = b_{coh\,X}^2 j_0^2(QR_X^{eq})(4\mathrm{e}^{-\gamma_{XX}Q^2} + 12\mathrm{e}^{-\gamma_{XX'}Q^2}) + 8 b_{coh\,X} b_{coh\,Y} \mathrm{e}^{-\gamma_{YX}Q^2} j_0(QR_X^{eq}) + b_{coh\,Y}^2 \mathrm{e}^{-\gamma_{YY}Q^2} \tag{52}$$

which is—to our knowledge—derived here for the first time, and generalizes the typically used expression [e.g. [15, 22]] for a rigid molecule.

Finally, to make practical calculations of $u(Q)$ and $v(Q, t)$ possible, an evaluation of the Debye–Waller coefficients (in the elastic case) or of the sums $\sum \langle z_{\nu\nu'} \rangle$ in equation (38) (in the inelastic case) for YX_4 molecules is needed.

If only zero-point vibrations can occur, one can refer to the Debye–Waller coefficients given in table 3, both for methane and its heavy twin. The treatment outlined by Pope [4] was followed here to calculate the reported values which, in the case of CH_4, slightly differ from the only ones reported by Griffing [8] (following Pope [4]) in the XX and YY case. This is partly due to the use here of the CH_4 mode frequencies provided by Herzberg [32], rather than those reported in [4]. Moreover, Rosenthal's method [36] for the force constants' determination was adopted here, both for CH_4 and CD_4. Another method was also reported by Pope [4] and [13] therein, and used there to carry out example calculations for methane. The way of deriving the force constants from available mode frequencies, and consequent slightly different values for the resulting Debye–Waller coefficients, is, however, not vital. In fact, we believe that differences in using one set or the other should anyway have a marginal effect on the calculated cross-sections, since both ways lead to a comparable value, for all the coefficients. These conclusions can be verified by a careful use of [4], with the warning that the third of equations (4.3) and most of the expressions in equation (6.1) of the quoted paper are wrong. By the way, it is worth mentioning that the values for the Debye–Waller coefficients of CD_4 are—to our knowledge—calculated here for the first time.

The $a_{\nu\nu'}$ data also shown in table 3, and equations (48) and (52), explain why the XX' and YX terms were neglected in previous calculations for CH_4 [8]. To a better level of accuracy, the authors of [26] considered the contribution of XX' and YX terms, though calculating the corresponding Debye–Waller coefficients of CH_4 with the approximation (see table 3) $\delta_X = 0$ [35], which corresponds to neglecting the anisotropic component in the equivalent oscillator treated by Pope. In contrast to methane, it is seen in table 3 that all the terms are equally important in the case of CD_4, as a consequence of the very different coherent to incoherent ratios for the two hydrogen isotopes.

In case vibrational modes can be excited by the neutrons, the sums $\sum \langle z_{\nu\nu'} \rangle$ in equation (38) can be evaluated by using equation (36) and the set of eigenvectors $e_{\nu\lambda}$ provided by Pope for each nucleus and each of the possible nine modes of the YX_4 molecule (with the normalization $\sum_\nu e_{\nu\lambda}^2 = 1$ for each mode).

Table 3. Debye–Waller coefficients for CH_4 and CD_4, calculated here by following the treatment proposed by Pope [4] in the case of zero-point motion. Numerical values of the cross-sections terms of equation (40) for the two systems are also reported.

Debye–Waller coefficient (zero-point vibrations) [4]	CH_4 (present work)	CD_4 (present work)
	$\gamma_X = 2.232 \times 10^{-3}$ Å^2	$\gamma_X = 4.014 \times 10^{-3}$ Å^2
	$\delta_X = 9.445 \times 10^{-4}$ Å^2	$\delta_X = 5.385 \times 10^{-4}$ Å^2
	$\gamma_Y = 0.8965 \times 10^{-4}$ Å^2	$\gamma_Y = 2.027 \times 10^{-4}$ Å^2
$\gamma_{XX} = 2(\gamma_X + \delta_X)$	6.353×10^{-3} Å^2	9.106×10^{-3} Å^2
$\gamma_{XX'} = 2(\gamma_X + 2\delta_X)$	8.242×10^{-3} Å^2	10.183×10^{-3} Å^2
$\gamma_{YX} = \gamma_Y + \gamma_X + 3\delta_X$	5.155×10^{-3} Å^2	5.833×10^{-3} Å^2
$\gamma_{YY} = 2\gamma_Y$	1.793×10^{-4} Å^2	4.054×10^{-4} Å^2
Cross-section terms of equation (40)		
a_{XX}	6.5277 b	0.6082 b
a_{YX}	−0.2488 b	0.4437 b
$a_{XX'}$	0.1399 b	0.4450 b
a_{YY}	0.4424 b	0.4424 b

5. Review of the most common applications

The expressions derived up to now for the inter- and intramolecular cross-sections surely represent the first, basic, step for calculations of the double-differential cross-section according to equations (4) and (5), which, as shown in equations (23) and (24), (31) and (38) or (39), can generally be rewritten as

$$\frac{\mathrm{d}^2\sigma}{\mathrm{d}\Omega\,\mathrm{d}\omega} = \frac{k_1}{k_0}\left[u(Q)S_d(Q,\omega) + \sum_{J_0 J_1 \upsilon_1 l} F(Q, J_0, J_1, \upsilon_1, l)S_s(Q, \omega - \omega_{J_0 J_1} - \omega_{\upsilon_0 \upsilon_1})\right] \tag{53}$$

with F taking different expressions according to the specific case. While the discussion of the model calculations using equation (53) for possible comparisons with the results of *inelastic* neutron scattering experiments will be postponed, the more important (i.e. 'application-rich') case of diffraction from molecular fluids is addressed now. To this aim, it is useful to remember that the single-scattering intensity measured in a neutron diffraction experiment as a function of the scattering angle θ is (see, e.g., [21–24])

$$I(\theta) = \Phi N \Delta\Omega \int_{\substack{-\infty \\ \theta=const}}^{\omega_0} \varepsilon(k_1)\frac{\mathrm{d}^2\sigma}{\mathrm{d}\Omega\,\mathrm{d}\omega}\,\mathrm{d}\omega \tag{54}$$

with ε the energy-dependent detector efficiency and Φ the incident neutron flux. Equation (54) reflects the fact that neutrons recorded, at each given angle, in a diffraction measurement are not discriminated in energy. Scattering events with all possible values of the exchanged energy will thus contribute to the measured signal at θ, following the sample scattering law $S(Q, \omega)$. If each scattering event were an exactly elastic process, then the diffraction intensity would be proportional to $\mathrm{d}\sigma/\mathrm{d}\Omega = \int_{\substack{-\infty \\ \theta=const}}^{\omega_0} (\mathrm{d}^2\sigma/\mathrm{d}\Omega\,\mathrm{d}\omega)\,\mathrm{d}\omega$ and would provide a 'direct' measure of the sought-for static structure factor. This can be deduced by noting that *for elastic scattering* ($k_1 = k_0$) the general relationship $Q = k_0[2 - (\omega/\omega_0) - 2(1 - \omega/\omega_0)^{1/2}\cos\theta]^{1/2}$ reduces to $Q = Q_{el} = 2k_0 \sin(\theta/2)$, thus making the condition $\theta =$ constant equivalent to $Q = Q_{el} =$ constant; and the combination of equations (54) and (4) gives, in the static

approximation [37], i.e. for $\omega/\omega_0 \ll 1$:

$$I_{`el'}(\theta) = \Phi N \varepsilon(k_0) \Delta\Omega \int_{\substack{-\infty \\ Q=const}}^{+\infty} \mathrm{d}\omega \frac{\mathrm{d}^2\sigma}{\mathrm{d}\Omega\,\mathrm{d}\omega}$$
$$= \Phi N \varepsilon(k_0) \Delta\Omega \{u(Q_{el})[S_{CM}(Q_{el}) - 1] + v(Q_{el}, 0)\} \quad (55)$$

where the CM static structure factor of a molecular system, $S_{CM}(Q) = \int_{\substack{-\infty \\ Q=const}}^{+\infty} S(Q,\omega)\,\mathrm{d}\omega = 1 + F_d(Q,0) = F(Q,0)$, was introduced. Note that the static structure factor is nothing but the zeroth frequency moment of $S(Q,\omega)$. In equation (55), the subscript '*el*' is intended to identify the intensity that would be measured in the ideal case of an elastic scatterer (indeed, the static approximation itself corresponds to 'elastic' scattering conditions).

It is well known that there is no elastic scattering from a liquid, as a consequence of the absence of correlations at infinite time. Thus, although the main contribution to the intensity in a diffraction experiment originates from quasi-elastic events with frequencies around the main peak of $S(Q,\omega)$, inelastic scattering events nevertheless influence the diffraction pattern recorded from a liquid, thus corrupting the *direct* relation between $I(\theta)$ and $S_{CM}(Q)$, which only holds for purely (ideal) elastic scatterers, as expressed by equation (55). It is clear also that the lighter the molecule is, the stronger is the effect of inelastic scattering processes.

In order to extract the static structure factor from neutron diffraction data, one therefore needs a way to derive from the measured intensity the limiting behaviour depicted in equation (55). Such a procedure is often addressed as 'inelastic correction'. To this aim, it is immediately useful to identify an additive inelastic correction with the quantity by which equation (54) differs from equation (55), i.e.

$$I(\theta) - I_{`el'}(\theta) = \left[\Phi N \Delta\Omega \int_{\substack{-\infty \\ \theta=const}}^{\omega_0} \varepsilon(k_1) \frac{\mathrm{d}^2\sigma}{\mathrm{d}\Omega\,\mathrm{d}\omega}\,\mathrm{d}\omega - I_{`el'}(\theta)\right] \equiv \Phi N \Delta\Omega \varepsilon(k_0) P(\theta), \quad (56)$$

which also allows one to rewrite equation (54) as

$$I(\theta) = \Phi N \varepsilon(k_0) \Delta\Omega \{u(Q_{el})[S_{CM}(Q_{el}) - 1] + v(Q_{el}, 0) + P(Q_{el})\}. \quad (57)$$

In equations (56) and (57) the correction function P was defined in units of barn sr^{-1}. A well-known method for the calculation of this correction was first proposed by Placzek [38] (that is also the reason why it is traditionally named P, meaning 'Placzek correction') and it is based on the series expansion of P in the frequency moments (of order higher than the zeroth one) of $S(Q,\omega)$, each calculated at $Q = Q_{el}$. An alternative approach for estimating P is to take advantage of the expression given in square brackets of equation (56), since its evaluation can be entrusted to the use of reasonable models for the (unknown) double-differential cross-section of the sample under study, as will be discussed in the following. Here, it might be helpful to remember that the use of models is anyway required even in the Placzek method, since only the first frequency moment of the dynamic structure factor is exactly known, while higher-order moments depend on $S(Q,\omega)$ itself. Further, the Placzek approach is expected to become inefficient as the mass of the system is reduced, because of the high number of terms in the moments expansion that should be retained.

On the whole, equations (54)–(57) immediately clarify why the model calculations treated in the previous sections represent an unavoidable ingredient in the analysis of neutron diffraction data from diatomic and other molecular fluids. In particular, in order to extract the sought-for function $S_{CM}(Q)$ from the measured intensity, one needs reasonable estimates for:

(i) the static inter- and intramolecular cross-sections, $u(Q)$ and $v(Q,0)$;
(ii) the inelastic correction $P(Q)$, which can be evaluated by taking advantage of the discussed modelling of the double-differential cross-section;

(iii) the normalization factor $\Phi\,\varepsilon(k_0)\,\Delta\Omega$, to be determined by comparing the true experimental output and the calculated differential cross-section, for a 'reference' sample.

In this last respect, eligible standards are those whose scattering response can be modelled to a high degree of accuracy, and which ensure, at the same time, minor alteration of the geometrical set-up when passing from the measurements on the sample of interest to those on the calibration sample.

The next subsections treat the above three basic applications.

5.1. The molecular self and distinct cross-sections in the static case

As was shown from equation (4) onwards, the distinct molecular term, $u(Q)$, is time-independent. As a consequence, it modulates, unaltered, both the static and dynamic intermolecular structure ($S_{CM}(Q)$ and $S_d(Q,\omega)$). The situation is different with the self molecular term. It is important to observe that, in the static version ($t = 0$) of equations (9), (28) and (32), one is mathematically allowed to use the completeness relation over the final molecular states. A consequence is that exact summation over the initial states, of appropriate probability, turns out in these conditions to be possible and leads to 'finite' expressions for the self molecular term in the various cases, which, however, correspond to a sum over *all* transitions. For this reason we will indicate such expressions with $v^{tot}(Q,0)$. In particular, for *diatomic molecules* it is found

$$v^{tot}(Q,0) = 2(b_{coh}^2 + b_{inc}^2) + (b_{coh}^2 - Rb_{inc}^2)\left[\int_{-1}^{1} \mathrm{d}\eta\, \mathrm{e}^{2\mathrm{i}\beta\eta}\mathrm{e}^{-2\alpha^2\eta^2}\right], \tag{58}$$

with $R = 0$ and $\frac{1}{2I}(1 - x_o/x_o^N)$, when spin correlations are, respectively, negligible or not, while for *spherical top* molecules with negligible spin correlations, the calculation of $\langle\langle 0|\, \mathrm{e}^{\mathrm{i}\boldsymbol{Q}\cdot\boldsymbol{x}_{\nu'}}\mathrm{e}^{-\mathrm{i}\boldsymbol{Q}\cdot\boldsymbol{x}_{\nu}}|0\rangle\rangle_\Omega$ and of the rotational part, leads to

$$v^{tot}(Q,0) = 4a_{XX} + a_{YY} + 8a_{YX}\mathrm{e}^{-\xi_{YX}Q^2}\, j_0(QR_X^{eq}) + 12a_{XX'}\mathrm{e}^{-\xi_{XX'}Q^2}\, j_0\left(Q\sqrt{\tfrac{8}{3}}R_X^{eq}\right) \tag{59}$$

where

$$\xi_{\nu\nu'} = \sum_\lambda \frac{\hbar}{12\omega_\lambda}\left(\frac{e_{\nu\lambda}^2}{m_\nu} + \frac{e_{\nu'\lambda}^2}{m_{\nu'}} - \frac{2\boldsymbol{e}_{\nu'\lambda}\cdot\boldsymbol{e}_{\nu\lambda}}{\sqrt{m_{\nu'}m_\nu}}\right),$$

which vanishes if $\nu = \nu'$.

Though $v^{tot}(Q_{el},0)$ is often employed in equations (55) and (57) in place of $v(Q_{el},0)$, it is clear that care must be taken in the use of equations (58) or (59) for experimental data analysis whenever the thermodynamic conditions of the fluid and the neutron incident energy are not able to activate some of the dominant transitions. In all those cases in which a limited number of transitions is enabled (because of temperature, neutron energy or both) a better accuracy is assured by using the *partial* sum obtained by specific calculations of (see, e.g., equation (23) at $t = 0$)

$$v(Q_{el},0) = \sum_{J_0 J_1 \upsilon_1 l} F(Q_{el}, J_0, J_1, \upsilon_1, l) \tag{60}$$

over the *possible* transitions only, strictly depending on the (known) experimental conditions.

Figures 1 and 2 clearly show that in rather common experimental conditions important differences may arise between v and v^{tot}, especially for the hydrogen compounds (H_2 and CH_4) and, generally, with increasing wavevector transfer. This last feature is a consequence of the increasing importance of high l terms (related to Bessel or similar functions) at high Q values, which do not contribute to v, unless many high-order transitions are enabled. As one

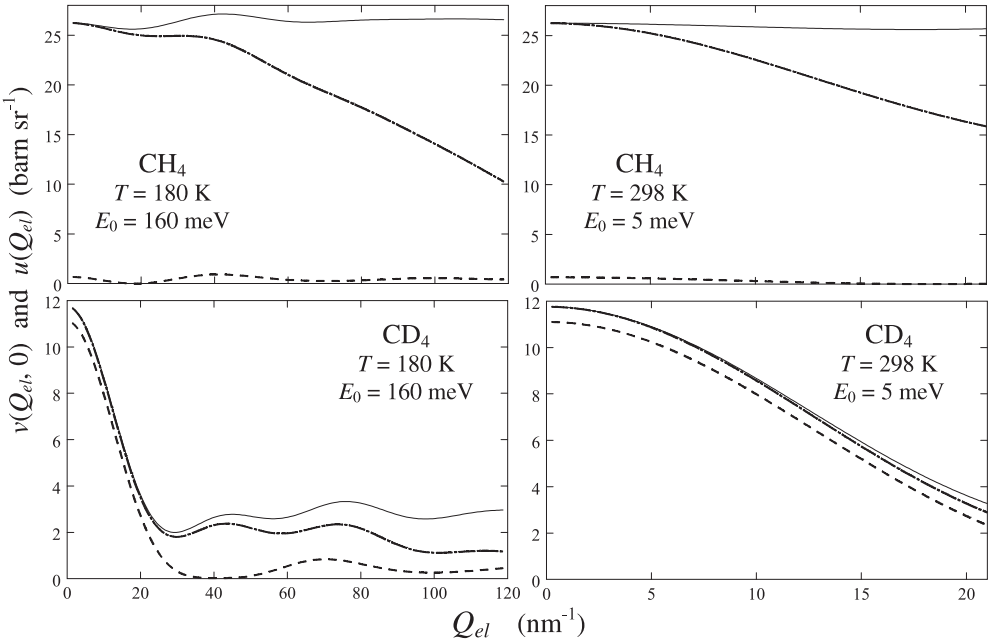

Figure 1. Example calculations of $v(Q_{el}, 0)$ and $u(Q_{el})$ for methane and deuteromethane in different experimental conditions. The full curve corresponds to $v^{tot}(Q_{el}, 0)$ according to equation (59), while the chain curve is $v(Q_{el}, 0)$, resulting from the sum in equation (60) over the admitted transitions at a given temperature T and neutron energy E_0 (see also equation (48)). The broken curve is $u(Q_{el})$, derived from equation (52).

would expect, at given Q and T, differences are more pronounced at lower incident energies, as a result of the smaller number of transitions excited by the neutrons (see, e.g., the D_2 case in figure 2) and contributing to v. The same consideration would apply at lower temperatures, at given E_0 and Q (because most molecules lie initially only in the lowest rotational levels). A case of particular importance is described in detail in figure 2, in connection with the *para*-hydrogen case at liquid temperature. There, v not only differs markedly from v^{tot}, but this difference changes dramatically when E_0 is below the activation threshold of the first rotational transition ($J_0 = 0 \rightarrow J_1 = 1$). In such conditions, in fact, the effects of the huge incoherent cross section of hydrogen are frozen, while only the very small coherent cross-section is left to weigh the various terms in v. Finally, it is clear, from figures 1 and 2, how the intermolecular cross-section, $u(Q)$, is far smaller than the intramolecular one, whenever hydrogen comes in. This obstacle, added to other difficulties, prevented neutron experimentalists to access the static structure of H_2 for a long time, until very recently [25]. An exception occurs for *para*-hydrogen at $E_0 < 15$ meV, where, though not shown for clarity in figure 2, $u(Q)$ is found to be comparable with the plotted v. Conversely, when deuterium is involved, the self and distinct cross sections are of the same order of magnitude, at least at low and intermediate Q. One of the main features of $u(Q)$—in all systems—is, however, its vanishing amplitude at finite Q values. The zeros of $u(Q)$ unavoidably prevent one to extract the CM structure factor in the vicinity of such Q values (see equation (57)). Fortunately, these often occur at high enough Q, so that the main features of the intermolecular structure can still be derived from the diffraction patterns (for comparison, a typical value for the Q position of the maximum in the static structure factor of molecules is 20 nm^{-1}).

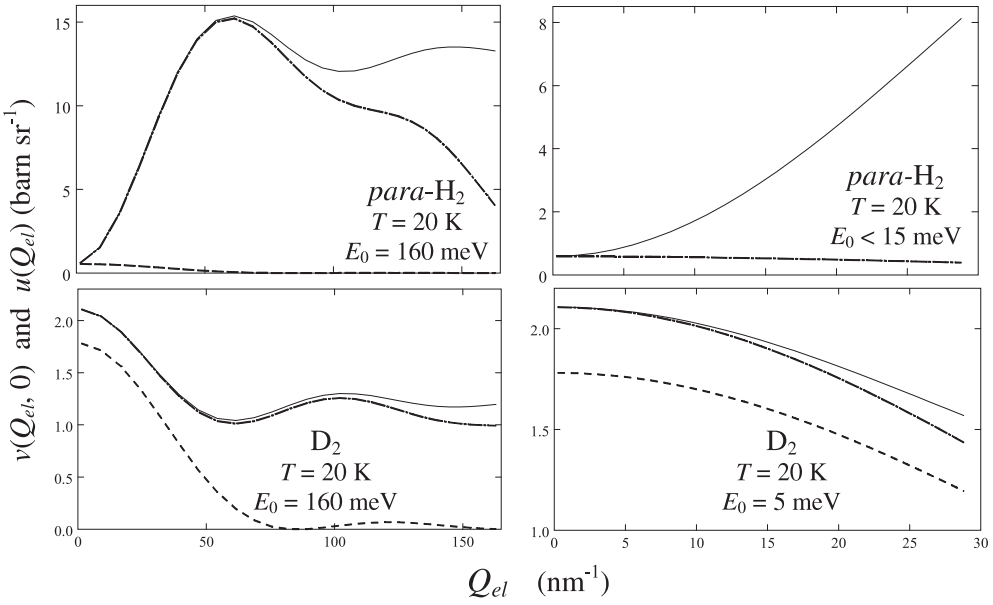

Figure 2. Example calculations of $v(Q_{el}, 0)$ and $u(Q_{el})$ for *para*-hydrogen and normal deuterium in different experimental conditions. The full curve corresponds to $v^{tot}(Q_{el}, 0)$ according to equation (58), while the chain curve is $v(Q_{el}, 0)$, resulting from the sum in equation (60) over the possible transitions at a given temperature T and neutron energy E_0 (see also equation (24)). The broken curve is $u(Q_{el})$, derived from equation (27). In the case of *para*-H_2 with $E_0 < 15$ meV, $u(Q)$ is not shown for the sake of picture clarity.

5.2. Evaluating the inelastic correction for some molecular fluids

As suggested previously, one possible way for estimating the correction function P in equation (57) relies on the assumption of a model for the double-differential cross-section of the sample and the evaluation of the corresponding quantity in square brackets in equation (56). In reactor-based diffraction experiments, such as those we are dealing with here, the inelastic scattering mainly affects the high-Q part of the diffraction pattern. At large Q values, the intermolecular structure decays and the system response tends to the perfect gas one, with $S_{CM}(Q) \approx 1$. It is then reasonable, in evaluating the inelasticity correction, to assume the simplest model available for the CM dynamics, i.e. the *ideal gas* (i.g.) one, which corresponds to

$$S_d^{i.g.}(Q, \omega) = 0$$

and

$$S_s^{i.g.}(Q, \omega) = \sqrt{\frac{M}{2\pi k_B T Q^2}} \exp\left[-\frac{M}{2k_B T Q^2} \left(\omega - \frac{\hbar Q^2}{2M} \right)^2 \right]. \tag{61}$$

When dealing with diffraction on diatomic and spherical-top molecules, it is therefore possible to exploit the expressions given before for the double-differential cross-section and, through the use of the above modelling of $S(Q, \omega)$, calculate the inelasticity correction for the system of interest as if it were an ideal gas of (rotating and vibrating) molecules. In this case, one

obtains (see equation (56))

$$\left[\Phi N \Delta\Omega \int_{\substack{-\infty \\ \theta=const}}^{\omega_0} \varepsilon(k_1) \frac{\mathrm{d}^2\sigma}{\mathrm{d}\Omega\,\mathrm{d}\omega} \mathrm{d}\omega - I_{el}(\theta)\right]_{i.g.} = \Phi N \Delta\Omega \varepsilon(k_0) P(Q_{el})_{i.g.} \tag{62}$$

with

$$P(Q_{el})_{i.g.} = \int_{\substack{-\infty \\ \theta=const}}^{\omega_0} \frac{\varepsilon(k_1)}{\varepsilon(k_0)} \left(\frac{\mathrm{d}^2\sigma}{\mathrm{d}\Omega\,\mathrm{d}\omega}\right)_{i.g.} \mathrm{d}\omega - v(Q_{el}, 0), \tag{63}$$

where equation (55) for an ideal molecular gas ($S_{CM}(Q) = 1$) was used, and the subscript at the double differential cross-section means that calculations are carried out by inserting the ideal gas $S(Q, \omega)$ (equation (61)), appropriately shifted in frequency, into the general expression given in equation (53).

It has been shown that such a simple approach accounts fairly well for the inelastic scattering correction even in the case of diffraction measurements on molecular liquids as light as deuterium [21]. Figure 3 reports, for example, the calculated $P(Q_{el})_{i.g.}$ for three realistic cases: (a) liquid deuterium at 20.7 K and $E_0 = 162.3$ meV [21]; (b) gaseous CD_4 at 180 K and $E_0 = 162.3$ meV [23]; (c) gaseous chlorine at 405 K and $E_0 = 13.9$ meV [39]. For the evaluation of the inelasticity correction of Cl_2, the diatomic uncorrelated-spin picture discussed in subsection 3.2 (which also neglects anisotropic components in the intermolecular interaction) was adopted.

In figure 3, calculations are compared with the '*effective*' inelastic correction, P^{eff}, resulting from an alternative data treatment based on fits of equation (57) to the high-Q portion of the experimental intensities (see, e.g., [21, 23] for details). In the case of chlorine (which is the heaviest system considered in the present examples), only one curve is shown, since the calculated and effective corrections were found to coincide. For the CD_4 example, the incident energy was such to enable 'one-phonon' vibrational transitions (the energy of the ground vibrational state of CD_4 is [4, 32] $\sum_\lambda \frac{1}{2}\hbar\omega_\lambda = 865.07$ meV). In particular, with 160 meV incident neutrons, the two (degenerate) modes of frequency 1054 cm^{-1} (130.68 meV) and the three (degenerate) modes of frequency 996 cm^{-1} (123.49 meV) can be excited. Therefore the calculations were performed using the treatment proposed in section 4, with five possible final sets $\{n_{\lambda,1}\}$ plus that corresponding to the ground state. For comparison, the calculation in the case of zero-point vibrations only ($P^{(0)}$) is also shown.

Both in the case of deuterium and of deuteromethane, the effective correction is less structured than the calculated one and turns out to have a different intensity. It must be noted, however, that the way in which P^{eff} is usually derived does not ensure a full independence of this quantity from other corrections of the diffraction data, such as multiple scattering (which is often evaluated in the elastic approximation) and background subtraction. Therefore, the resulting P^{eff} might compensate also for residual effects which do not originate from single inelastic scattering. On the other hand, it is important to remember that a rather accurate knowledge of the experimental detector efficiency, $\varepsilon(k_1)$, would be required in order to carry out realistic calculations of equation (63). Unfortunately, it is nearly impossible to achieve detailed information on the true detector performance, and calculations can only rely on an approximate evaluation of it, based on the well-known expression $\varepsilon(k_1) = 1 - \exp[-a(k_0)k_0/k_1]$, with $a(k_0)$ being an absorption coefficient depending on the specific detector. Given such uncertainties, the results of figure 3 are, on the whole, satisfactory, since the correct order of magnitude for the inelastic correction is derived from the calculations.

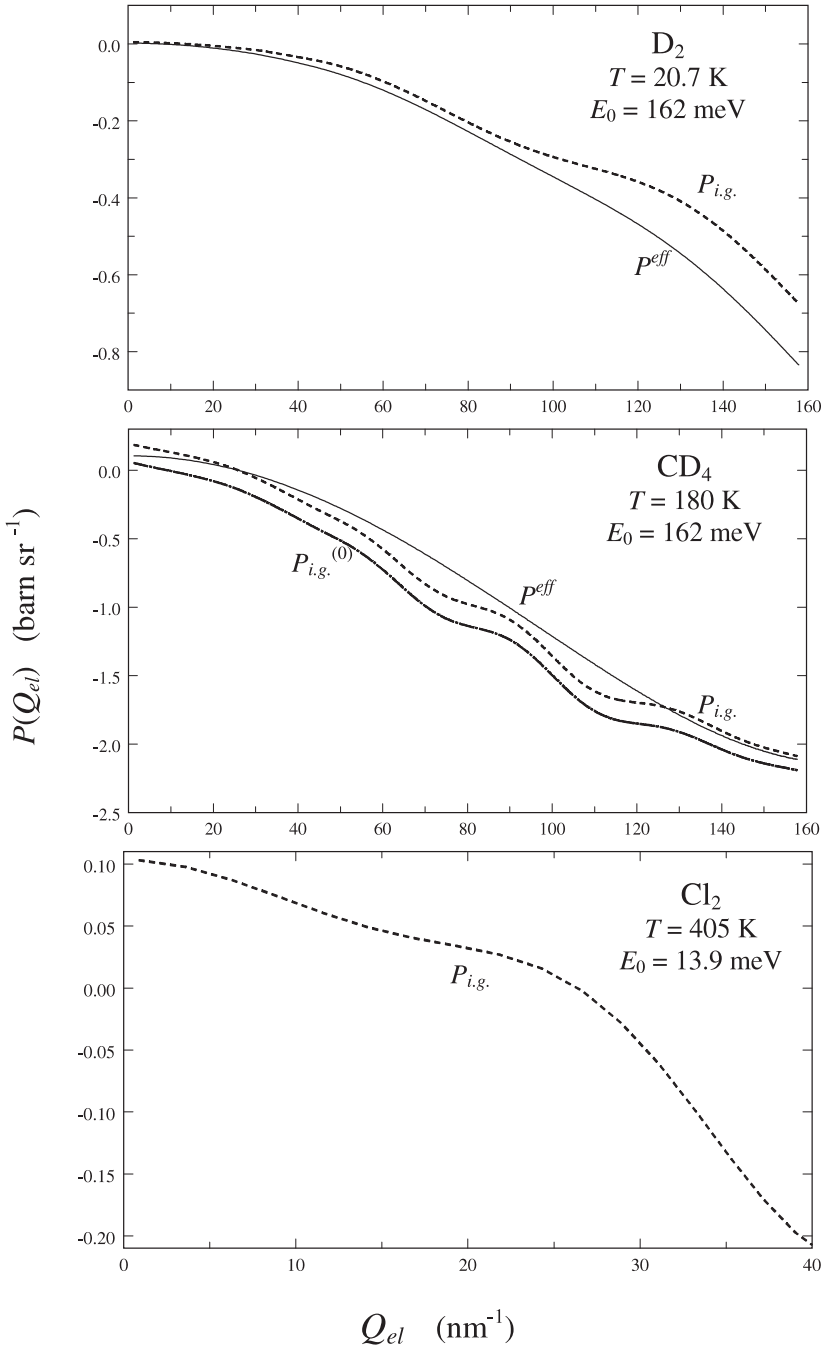

Figure 3. Example calculations of $P(Q_{el})_{i.g.}$ according to equation (63) for D_2, CD_4 and Cl_2. The calculated inelastic correction (broken) is compared with the effective one (full) derived by different data analysis (see the text). In the case of chlorine, calculations are found to provide the effective correction required, without the need of modifications. In that of CD_4, comparison is also made between $P^{(0)}$ (chain), accounting for zero-point motions only, and P including also the 'one-phonon' scattering events (see the text) enabled by the high incident energy of the present example.

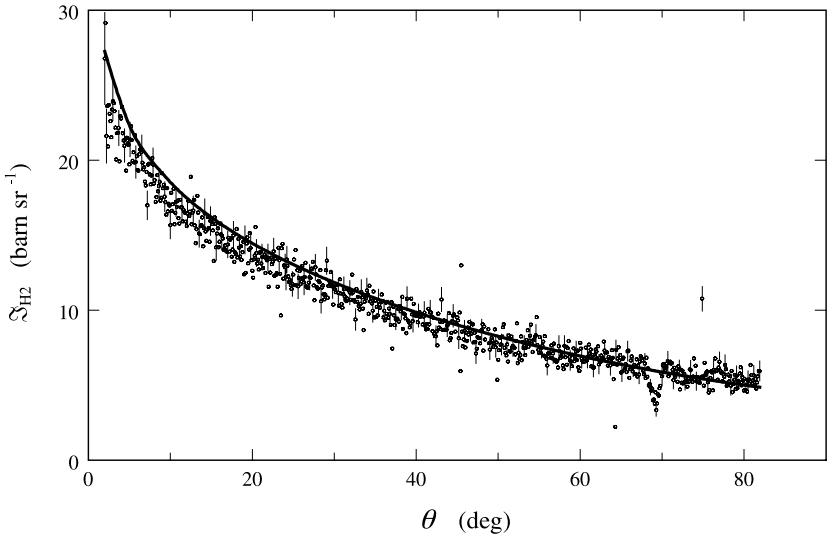

Figure 4. The differential cross-section $\Im$ of low-density hydrogen at room temperature and 13.9 meV incident energy. Experimental data collected on the G.4.1 diffractometer of LLB, after vanadium normalization (circles with error bars) and corresponding calculation based on the ideal gas model for the translational dynamics (full curve).

5.3. Neutron diffraction data normalization

The use of incoherent molecular gases, such as H_2 and CH_4, for neutron data calibration was introduced quite recently [26–28], with the aim of minimizing possible errors in the determination of the instrumental factor $\Phi\varepsilon(k_0)\Delta\Omega$, mainly originating from geometrical differences between a fluid sample and the standard (vanadium, typically). The clear advantage, from the experimental side, lies in the possibility of using the same container both for the sample and for the reference gas and, generally, without the need to remove the container from its position in the beam.

This method is applied by recording the diffraction intensity from a very low-density sample of hydrogen or methane (i.e. close to ideal gas conditions), and by comparing it with the computed differential cross-section, following the models described in the previous sections 3 and 4 when the ideal gas $S(Q, \omega)$ is assumed as the CM scattering law. In formulae ($R = H_2$ or CH_4)

$$\Phi\varepsilon(k_0)\Delta\Omega = \frac{I(\theta)_R^{expt}}{N_R \int_{\substack{-\infty \\ \theta=const}}^{\omega_0} \frac{\varepsilon(k_1)}{\varepsilon(k_0)} \left(\frac{\mathrm{d}^2\sigma}{\mathrm{d}\Omega\,\mathrm{d}\omega}\right)_{R,i.g.} \mathrm{d}\omega}. \tag{64}$$

For ease of notation, $\Im_R$ will indicate, in the following, the frequency integral at the denominator of equation (64).

As an example of the results attainable by this joint use of experiment and calculation, it is significant to compare (see figure 4) the calculated $\Im_{H_2}$, with its experimental equivalent, derived by vanadium normalization of the single scattering intensity from a dilute hydrogen sample. Experimental hydrogen data refer, in particular, to a room temperature measurement performed on the G.4.1 diffractometer of Laboratoire Leon Brillouin (LLB), with $E_0 =$ 13.9 meV.

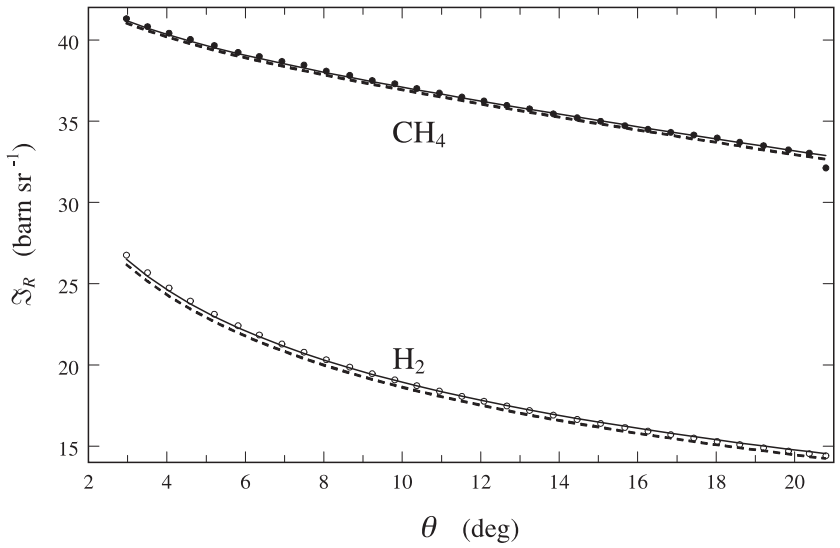

Figure 5. The differential cross-section of low-density hydrogen and methane at room temperature and 4.9 meV incident energy. Calculations of $\Im$ (as in equation (64)) were performed using both the nominal detector efficiency (49% at 4.9 meV, broken curves) and by assuming a higher performance (60% at 4.9 meV, full curves). Dots (for methane) and circles (for hydrogen) represent the effective $\Im$—derived from the experimental intensities—able to give full agreement between the low-Q extrapolation of the measured $S(Q)$ and the $S(0)$ compressibility limit of a Kr sample at room temperature and number density 4.3 nm^{-3} [28].

The agreement between data and calculations in figure 4 is, indeed, very good. The shape, in particular, of the experimental differential cross-section (rising quite steeply with decreasing scattering angle) does not seem to support the widespread opinion regarding the unsuitability of *ideal gas* calculations for the representation of scattering data on fluid samples, especially at low incident energies and small angles (see, e.g., [18]). As a matter of fact, experiment and calculation give, in this case, nearly the same result, though with a very slight, but detectable, overestimate of the experiment by calculations when θ is decreased. Differences are anyway well within the experimental errors—at least at these intermediate incident neutron energies—which is important evidence, still missing up to now.

The accuracy of the calibration technique discussed here can be estimated from the results of figure 5, which refer to a small-angle experiment on a gaseous Kr sample [28]. There, the computed $\Im_R$ is compared with the one that would have given a perfect agreement between the low-Q behaviour of the experimental structure factor $S(Q)$, normalized using either a CH_4 or a H_2 measurement, and the $S(0)$ thermodynamic limit predicted from Kr compressibility data. If the nominal detector efficiency is employed in the calculations of $\Im_R$ (broken curves in figure 5) a 1 and 2% accuracy is obtained, respectively, with methane and hydrogen normalization. Agreement is even better if a higher efficiency is assumed (full curves in figure 5), though such an assumption has no convincing experimental reason. Nonetheless, it is interesting to note how the calculation for hydrogen is more sensitive to the choice of the detector efficiency and, for this reason, how the same increased value for the efficiency brings in very good agreement calculations and experimental quantities, both in the hydrogen and methane cases.

Finally, it is useful to observe that the better accuracy which seems to be attainable with methane is counterbalanced, from a practical point of view, by the unavoidably longer computing times required for this molecular system, especially with increasing E_0. This is due

to the far lower rotational constant of CH_4($B = 0.65$ meV) with respect to that of hydrogen ($B = 7.35$ meV): many more transitions must be considered for methane, at given incident energy and temperature. Therefore, the compromise between normalization accuracy and overall computing time appears to make the two standards (H_2 and CH_4) both very good and equivalent on the whole.

6. Inelastic neutron scattering data and calculations

Despite the considerable amount of work devoted to the prediction of the double-differential cross-sections of hydrogen and methane, suitable experimental data sets allowing for a reliable test of the computational results appear to be partly lacking in the literature. Comparison is often made difficult either because available data are not normalized to absolute units, or because large uncertainties lean upon the appropriate correction for important effects, such as multiple scattering, or, finally, because neither correction for energy resolution broadening was attempted on the spectra nor appropriate details on the instrumental resolution function given, especially in the earlier papers.

Concerning the hydrogens, coherent inelastic scattering measurements on liquid para-hydrogen and deuterium performed in the last decade [40], which would have been of some interest to analyse with the treated models (also in terms of the possible choices for the distinct dynamic structure factor $S_d(Q, \omega)$), are unusable for our purposes since data are never resolution-free (and the instrumental resolution function is not reported) nor normalized to absolute units. The only possible comparison, based on an assumed resolution, plus a reduction of data and calculations to the same integrated intensity, appears to be largely meaningless.

Further, no slow or thermal neutron scattering data appear to be available for the self (incoherent) double-differential cross-section of H_2. Conversely, an interesting comparison between deep inelastic neutron scattering (DINS) data and the model calculations outlined here, though modified to take into account quantum effects on the translational kinetic energy and anharmonicity of vibrations, at the very high momentum transfers relevant for DINS, has been performed in recent years [41] and will not be repeated here.

The situation is less critical with neutron inelastic data on methane, at least for the incoherent scattering. Existing data on CH_4 are, however, quite old [42–45] and usually suffer from the mentioned problem concerning energy resolution broadening [42, 43] and/or missing data normalization [44, 45]. Therefore, examples are limited here either to the comparison with normalized methane data [42, 43], whose energy resolution effects can be taken into account with some confidence, or with (unnormalized) low-E_0 measurements [45], i.e. affected by negligible resolution broadening.

Figure 6 reports the experimental neutron data for gaseous [42] and liquid [43] methane, at fixed scattering angles. Incident neutron energy and sample temperature are specified on each frame. Liquid methane data (figures 6(a)–(c)) are compared with the computed double-differential cross-section (per unit scattered wavelength) according to the model discussed in section 4, with two different choices for $S_s(Q, \omega)$: either the ideal gas model of equation (61) or the 'mixed model' proposed by Egelstaff and Schofield [46], later discussed also by Copley and Lovesey [47]. Such a model has the perfect gas form at high Q, and the simple diffusion behaviour at low Q, according to [47]

$$S_s(Q, \omega) = \frac{cQ^2D}{\pi\sqrt{\omega^2 + (Q^2D)^2}} \exp(cQ^2D) K_1\left(c\sqrt{\omega^2 + (Q^2D)^2}\right) \tag{65}$$

where $c = MD/(k_BT)$, with D the self-diffusion coefficient, and K_1 is the modified Bessel function of the *second* kind. Note that nearly all the papers reporting the model of equation (65)

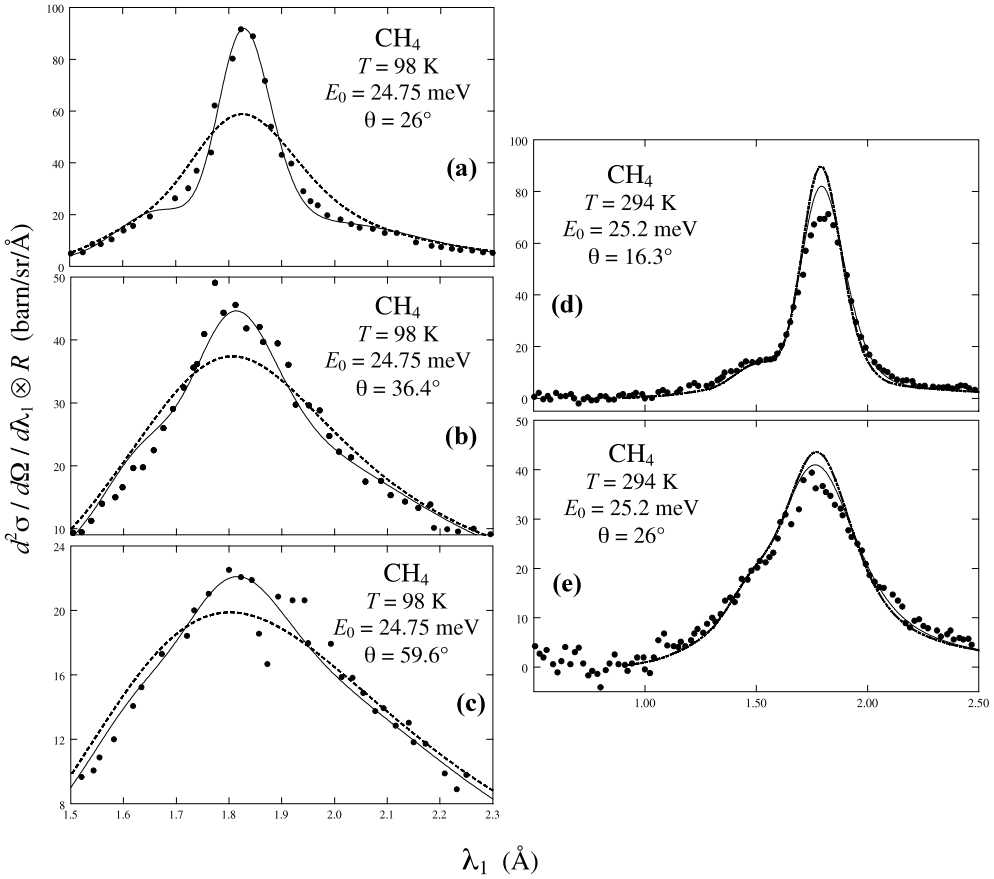

Figure 6. (a), (b), (c): liquid methane neutron data at different scattering angles of [43] (dots), compared with model calculations (section 4) using the ideal gas (broken curve) and the mixed model (full curve) proposed by Egelstaff and Schofield [46, 47], with $D = 2.7 \times 10^{-5}$ cm^2 s^{-1} [49], for the translational self-dynamics. Calculations were convoluted with a ∼1.5 meV Gaussian resolution function R in order to make the comparison with experiment possible (see the text). (d), (e): gaseous methane neutron data at two angles of [42] (dots), compared with the calculations performed with the ideal gas law for translations. Results with (full curve) and without (chain curve) correction for a ∼1.5 meV resolution are shown.

wrongly indicate K_1 as the modified Bessel function of the first kind, which, however, has not the required asymptotic behaviour. Further, since the above model is classical, the detailed balance condition has to be imposed before equation (65) is employed in the calculations. It has been shown [48] that this can be done in an approximate way by multiplying the classical $S_s(Q, \omega)$ by $\exp[(\hbar\omega/2k_BT) - \hbar^2Q^2/8Mk_BT]$.

In the calculations, the experimental value for the self-diffusion coefficient of CH_4, $D = 2.7 \times 10^{-5}$ cm^2 s^{-1} [49], was used. Moreover, as indicated also by Dasannacharya and Venkataraman in [44], the non-negligible effects due to energy resolution broadening on the data of [43] could be taken into account by a resolution width of ∼1.5 meV, which has thus been used for the convolution of the calculations with a Gaussian-shaped resolution function (R in the figure labels). The ideal gas calculations were also broadened, accordingly.

No special comments are required about the general agreement between liquid methane data and the present calculations using the mixed model of Egelstaff and Schofield.

The significance of earlier comparisons with the same data, which neglected resolution effects (see, e.g., [16]), is not clear.

Similarly to the satisfactory predictions for the liquid (once a reasonable model for S_s is adopted), it is found that in the gaseous phase (figures 6(d) and (e)) simple molecular ideal gas calculations are able to account reasonably for the experimental results.

Concerning the experimental spectra of [45], it is worth noting that, though erroneously labelled in units of barn sr^{-1} $\mu\mathrm{s}^{-1}$ m, both in the original paper and in [17], data are only relatively normalized. In fact, the reported values for the double-differential cross-section are not realistic and would provide (by integration) a differential cross-section, at each given angle, at least one order of magnitude greater than what it is known from diffraction experiments at similar incident energies (see, e.g., figure 5 at 20°). Therefore comparison with the present calculations (which are in absolute units) is performed by preliminary area normalization of the measurements of [45] to the computations, in the same range of neutron inverse velocity covered in the experiment. The slow neutron spectra [45] for gaseous CH_4 at room temperature and various scattering angles are shown in figure 7, together with the predictions based on the ideal gas $S_s(Q, \omega)$. Slight differences are observed at the lowest scattering angles, similarly to the case of figures 6(d) and (e), while extremely good agreement is found at higher angles. By comparison with the similar calculations reported in [45], a systematic and detectable improvement is observed with the present calculations, at all angles. This can be due to the various refinements introduced here, both concerning the Debye–Waller coefficients and the transitions taken into account.

7. Practical aspects in the computations

It is quite obvious that the two fundamental parameters ruling the development of the calculations are the temperature of the fluid and the incident neutron energy. The former determines the initial roto-vibrational state of the sample, while the latter defines the possible transitions. Some preliminary considerations are thus common to each calculation. A second phase regards, instead, specific implementation and program refinement according to the formulae given in sections 3 and 4, and depending on the systems under study (H_2, CH_4, Cl_2, etc).

It is understood that the simple remarks made in the following subsections (and the related appendix) are only meant to help neophytes interested in the model computations discussed.

7.1. Common features of the calculations

The models described here all assume as the initial vibrational state of the molecules the fundamental one ($\upsilon_0 = 0$, $p_{\upsilon 0} = 1$). This will hold if the thermal energy, $k_B T$, at the temperature under consideration is lower than the first excited vibrational state of the system. As a second step, the latter has to be compared with the incident neutron energy E_0, in order to establish whether vibrational transitions can or cannot be induced by the scattering process.

Similar comparisons must be carried out for rotations. In particular, once the rotational partition function has been calculated at the given temperature, the single state probabilities p_{J0} (see, e.g., equations (20) and (49)) must be analysed in order to decide how many rotational states are (significantly) thermally populated. In the examples given in the present paper, calculations were typically performed for $J_0 = 0, 1, \ldots, J_{0\,max}$, with $J_{0\,max}$ such that $p_{J0\,max} \sim 10^{-6}$. For each J_0 taken into consideration, one has then to determine the possible final states, J_1. If the neutron energy is so low that no transition is allowed towards higher rotational states, then J_1 will vary between 0 and J_0 (i.e. anti-Stokes transitions only can

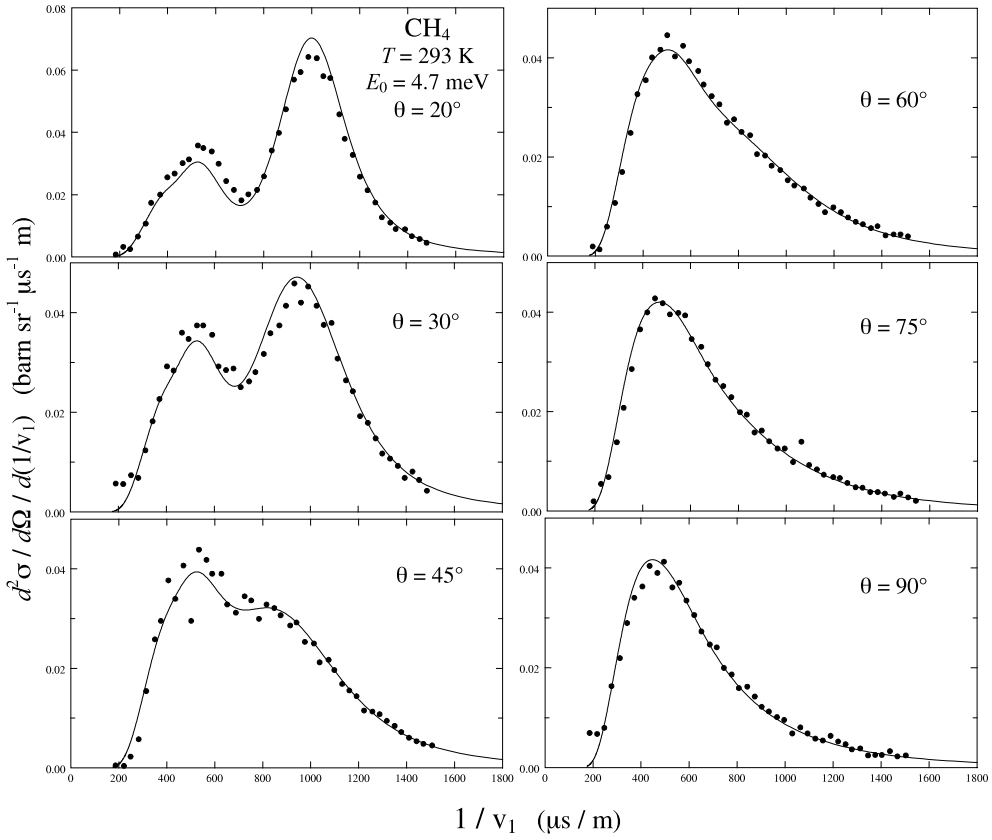

Figure 7. Gaseous methane slow-neutron data at various angles of [45] (dots), compared with the calculations performed with the ideal gas law for translations.

occur), else the incident energy value will be used to establish the maximum J_1 that can be reached, starting from a given J_0. In this case, all those final levels satisfying the condition $E_{J0J1} = E_{J1} - E_{J0} \leqslant E_0$ must be considered, and J_1 will vary in general between 0 and $J_{1\,max}(J_0)$ (i.e. Stokes and anti-Stokes transitions take place).

It is clear that, in terms of computing time, the situation gets progressively worse with increasing temperature (many rotational levels are significantly populated) and incident energy (many transitions are enabled), and with increasing the mass of the system (a lower rotational constant B corresponds to smaller E_{J0J1}, and, thus, to more Stokes transitions, if possible). Moreover, the larger the number of transitions, the harder becomes a smooth calculation of the various quantities present in the models, such as the CG coefficients and the integrals A_{l,υ_1} (or, similarly, the spherical Bessel functions j_l), without running into easy problems related to insufficient stack space, or unacceptable computing time, or overflow, or, finally, rounding or integration errors. Part of these difficulties are nowadays by-passed with the powerful mathematical tools provided by most commercial software. However, a good compromise between available functions and their efficient use in programs written under such packages is still missing, mainly because these are often quite slower than similar programs written in other languages. A possible approach is to take advantage of the quick and accurate evaluations which are possible today for the quoted functions (Bessel functions, Legendre polynomials, etc) by performing

their preliminary calculation in the required conditions (depending, however, on each transition involved and each Q–ω point), and storing them in files to be used as inputs for more efficient programs for the calculation of the double-differential cross-section. Indeed, this is found to be quite an effective procedure, making the calculations generally possible in a reasonable time, even with a large number of transitions, several scattering angles, and narrowly stepped ω intervals. In addition, this avoids the—always uncomfortable—use of libraries. Of course, it is not always necessary to pass through the two-step calculation suggested above. In fact, the general implementation of simpler conditions (limited number of transitions) usually requires nothing other than completely standard computing tools (i.e. no special software), provided the overall accuracy of the various functions' evaluation is closely verified when their arguments are varied.

7.2. Special features of the calculations

While suggestions related to the specific functions entering the models can be found in the appendix, a final hint for the accurate development of the diffraction case, as well as some advice for the inelastic one in demanding conditions, are given in the following.

7.2.1. The differential cross-section $\mathrm{d}\sigma/\mathrm{d}\Omega$. Some applications discussed here involve the use of the differential cross section, once the double-differential one has been modelled. More precisely, the evaluation of the integral $\Im$ present in equation (64), and including the detector efficiency, is often required. Thus, after the double-differential cross-section has been calculated, one needs to also perform its numerical ω integration. This further step is generally simple, provided that the lower bound of the integration range ($-\infty$, namely) is verified, as well as the integration step.

In fact, the shape and ω extension of the integrand is highly variable with changing the conditions in which the calculation is performed (E_0, T, M, θ). Therefore, it is mandatory both to check that the integrand is sampled with sufficient accuracy over the whole integration interval (i.e. that the integration step is small enough) and that the integrand is evaluated down to low enough ω, where one can be confident that its contribution to the integral has become negligible. If, in given conditions (M, T and E_0 fixed), the integration needs to be performed at various scattering angles, a safe procedure is to look initially at both the high- and low-θ behaviour of the double-differential cross-section (including efficiency). This will help in identifying suitable values for the sampling step and lower ω bound, able to ensure an accurate integration at all the angles of interest, and allowing for the implementation of an automatic, but reliable, calculation with varying θ.

7.2.2. An example for an exacting case: chlorine at high temperature. Due to the considerable mass of chlorine, the rotational constant B for this diatomic molecule is very low (0.0302 meV). This, if combined with a rather high temperature and relatively energetic neutrons, makes the number of possible transitions very high. If one is interested in the calculation of the isotropic approximation for the double-differential cross-section of this molecule (for instance, for the inelastic scattering correction in diffraction experiments, see section 5.2), then all the quoted difficulties, related to high l values in the evaluation of the CG coefficients (see, e.g., the appendix) and the integrals A_{l,υ_1}'s, will arise.

As an example, we may focus on the case of chlorine at 405 K and 14 meV incident neutron energy: more than one hundred rotational levels are non-negligibly populated at this temperature. Moreover, the above neutron energy is such that at least one Stokes transition (however, there can be as many as twenty, if J_0 is low) is enabled for each J_0. In addition, all anti-Stokes transitions are active anyway. Consequently, l values exceeding 200 should, in

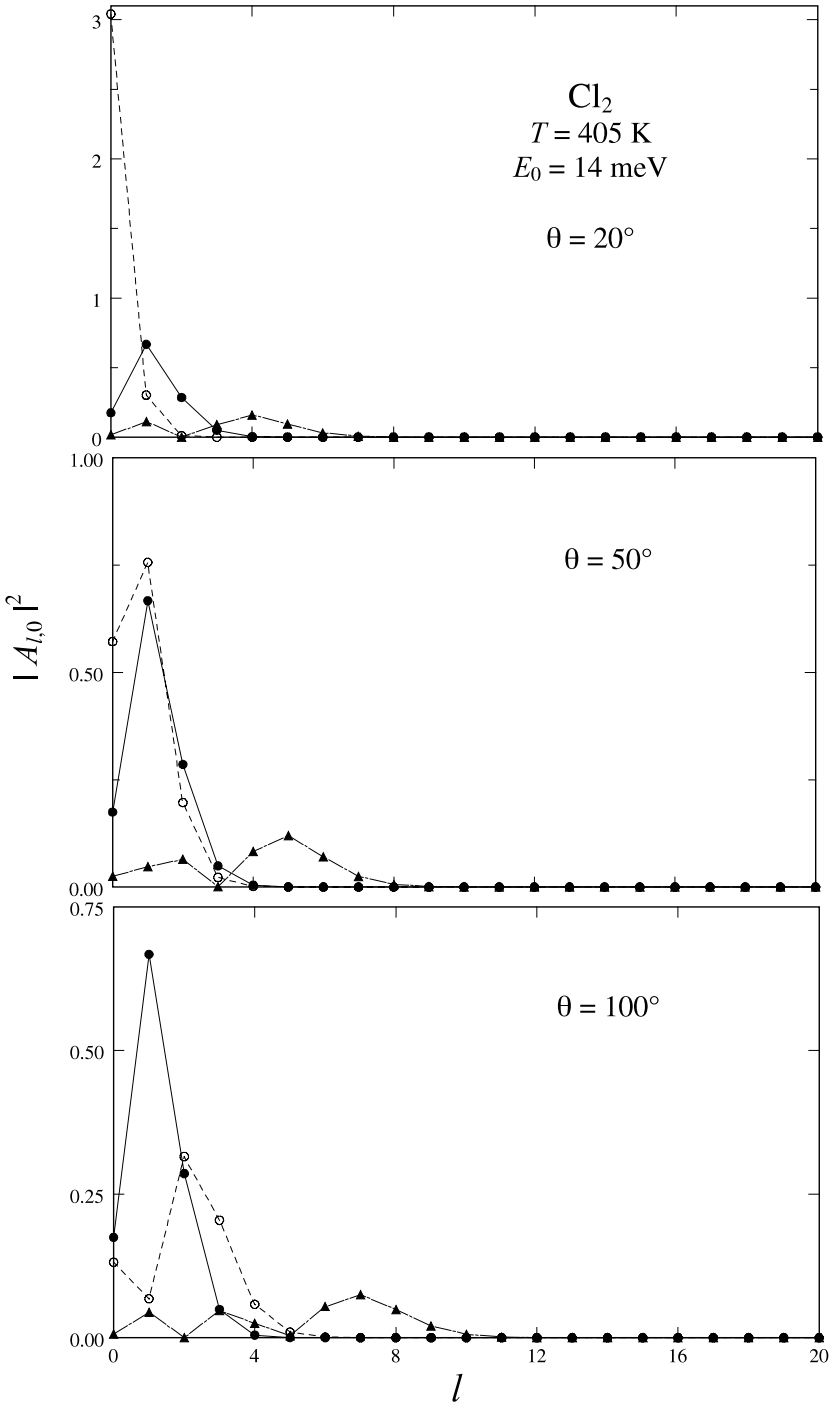

Figure 8. Importance of the square modulus of the integrals $A_{l,0}$ as a function of l, at three different scattering angles, for the case of chlorine at 405 K and 14 meV neutron energy. For each angle, the curves corresponding to three different values of ω are shown: $\omega = \omega_0$ (dots joined by a full curve), $\omega = 0$ (open circles joined by a broken curve), and $\omega = -195$ ps^{-1} (triangles plus chain curve).

principle, be considered. Of course, the main difficulty in these cases is the computing time, particularly because an accurate evaluation of the A_{l,υ_1} integrals requires a very narrow step at high l values. It is, however, useless to carry out the complete sum over all occurring l, since these integrals give a negligible contribution when l is high. An example is given in figure 8, where $|A_{l,0}|^2$ for chlorine in the quoted conditions can be analysed as a function of l, at three different scattering angles. The behaviour of $|A_{l,0}|^2$ at low, intermediate and high energy transfers is shown for each angle. From figure 8 it is clear that calculations can be limited to $l = 15$, without losing important contributions. This was also specifically verified, at the level of the double cross-section output, by comparison with a longer run where l values up to 30 were considered.

8. Final notes

Applications in the field of neutron diffraction data analysis, including a rather recent normalization technique, require both a reliable and efficient calculation of the double-differential cross-section of some molecules. The main steps and approximations allowing for practical computations were summarized here for basic cases. Generalization to other similar systems or conditions can be accomplished easily. The increased power of computing and mathematical tools available now is shown to provide an extremely significant contribution to the accuracy attainable with such calculations, especially if supported by a careful step by step verification.

As a matter of fact, really 'user-friendly' models for these calculations still appear not to differ too much from what was already suggested 40 years ago. Indeed, not too exacting refinements can be proposed, as well as extensions of the calculations—only possible with modern tools—which undoubtedly lead, as was shown in this paper, to significant improvements in the agreement between neutron experimental data and calculations. For instance, quite a step forward was made here in the treatment of some vibrational transitions for spherical-top molecules, without losing the simplicity and feasibility of the corresponding computations.

A more than satisfactory picture of the experimental findings, both for the double- and the single-differential *self* cross-section of these molecules, is ensured by the proposed computing procedures. A very high (2%) reliability is reached, for instance, in neutron diffraction data normalization using hydrogen or methane calculations.

Quite a non-negligible interest would cover the comparison of the reported model calculations with—thermal or slow—neutron inelastic scattering data from liquid or gaseous H_2 (in absolute units and with detailed energy resolution information), though such a 'simply fundamental' measurement is probably (and regretfully) only moderately appealing for today's experimentalists.

Open problems related to the slight inadequacies of the available models for the description of CH_4 inelastic scattering at small angles (sometimes identified with a possible sign of intramolecular vibration–rotation coupling) would as well require new accurate data, duly normalized and furnished with a precise knowledge of the experimental resolution function.

Acknowledgments

The author is indebted to U Bafile for extremely useful discussions and a critical reading of the manuscript, as well as to R Magli for collaboration on a large part of the experimental work used for comparison with the present calculations. S Pronti is acknowledged for general support

and prompt technical solutions. Part of this work was possible thanks to the unforgettable teachings of Peter Verkerk.

Appendix. Technical details and useful parameters

A.1. Clebsch–Gordan coefficients

In order to carry out the diatomic case, with or without spin correlations, the CG coefficients $C^2(J_1 J_0 l; 000)$ have to be calculated for each possible J_0, J_1 and l. This is quite straightforwardly done using a special case of the *Racah formula* (see, e.g., [33] vol II, equations $C.23(a)$ and $C.23(b)$) and the relation between squared CG coefficients and squared $3j$ symbols for this case, i.e.

$$C^2(J_1 J_0 l; 000) = (2l+1)\begin{pmatrix} J_1 & J_0 & l \\ 0 & 0 & 0 \end{pmatrix}^2. \tag{A.1}$$

As already mentioned, the above CG coefficients are zero whenever $J_1 + J_0 + l$ is odd. The non-zero coefficients are usually computed without problems, if the required factorials entering the quoted Racah formula are not too large. If transitions, and therefore factorials, grow to the extent that standard programming fails, one can resort to the use of the *gamma function*, usually available in commercial mathematical software, and having the property $\Gamma(x+1) = x!$. Since the natural logarithm of Γ is usually the default output, the CG coefficients involving high factorials can be reduced to the calculation of the exponential of an algebraic sum of logarithms of gamma functions of appropriate argument (each depending on the rotational quantum numbers, as defined by the Racah formula).

A.2. Spherical Bessel functions j_l

In analogy with what was discussed already at the end of section 3.1 for the integrals $A_{l,v}$, a correct calculation of high-order spherical Bessel functions by standard tools is an equally delicate matter. An important well-known warning concerns the use of the recursion relation typically reported for these functions, which gives wrong results when l exceeds the first 10 iterations, approximately. A much more reliable evaluation can be performed through the series definition given in [50] or by separate use of specific mathematical software. When many J_0, J_1 couples (and, consequently, l values) must be considered, the latter is not an easy route: mainly because of too much data to be stored and, then, to be read by other programs for *each* ω value and *each* scattering angle. In these cases, approximations appear to be unavoidable, which will reduce the overall computing time to acceptable limits.

Performing the calculations with a reduced maximum l is, however, not critical, since all the tests performed in this direction were successful in our experience, provided the upper l limit employed in the calculations is verified in some way. For instance, this can be done by comparing the output of a few long runs (i.e. without approximations), in selected conditions (e.g. low and high Q), with that of corresponding short runs, using limited l values.

As an example, the case of CH_4 at room temperature and 25 meV incident energy, can be reported: 24 initial rotational levels were considered, as well as consequent final rotational states, determined by E_0 (giving rise to Stokes transitions up to $J_0 = 18$). Various tests confirmed that nearly exact calculations could be reproduced also by limiting the Bessel function's evaluation to $l = 20$ (while l could reach even 48, in principle).

Table A.1. Basic quantities (rotational constants, equilibrium distances and vibrational mode energies) used in the present calculations for hydrogen(s), methane(s) and chlorine.

	H_2	D_2	Cl_2	CH_4	CD_4
B [32] (meV)	7.355	3.708	0.030	0.651	0.328
D [32] (meV)	0.0057	0.0014			
R_{eq} [32] / R_X^{eq} [51] (Å)	0.741 44	0.741 52	1.988	1.084	1.086
$\hbar\omega_\nu$ [32] (meV)	515.92	371.16	69.047		
$\hbar\omega_\lambda$ [4, 32] (meV)					
$\lambda = 1$				361.29	258.51
$\lambda = 2$				189.20	130.68
$\lambda = 3$				189.20	130.68
$\lambda = 4$				374.43	279.95
$\lambda = 5$				374.43	279.95
$\lambda = 6$				374.43	279.95
$\lambda = 7$				161.92	123.49
$\lambda = 8$				161.92	123.49
$\lambda = 9$				161.92	123.49

A.3. Legendre polynomials

Indeed, the calculation of the Legendre polynomials by the well-known recursion relation

$$P_l(x) = \frac{(2l-1)x\,P_{l-1}(x) - (l-1)\,P_{l-2}(x)}{l}, \tag{A.2}$$

presents no particular problems, holds up to high l values, and is easily implemented in any program. In order to reduce the overall computing time (if many evaluations are required as a function of the argument) it might be convenient to store them initially. In fact, it is useful to remember that, in the diatomic case, the Legendre polynomials appear in the integrands of the A_{l,υ_1}'s, whose accurate numerical integration might, sometimes, require a very narrow integration step $\Delta\eta$, and consequently many P_l evaluations.

A.4. Modified Bessel function of the second kind

As discussed in section 6, a possible model for the translational self dynamics is the Egelstaff and Schofield one (equation (65)), which requires evaluation of the modified Bessel function of the second kind, K_1, for each scattering angle, each ω value and each transition (remember equation (53)) involved in the calculation. Once again, the most efficient way to do this, nowadays, is to store the needed arguments (as a function of ω, transition and angle), and then calculate and re-store K_1 by available mathematical software. A main program reading such files may be implemented easily.

It might be useful to note, however, that for high arguments K_1 tends to zero. This condition makes the model of equation (65) fail—at least in a 'numerical' treatment—whenever D is high, as happens for gases ($D \sim 10^{-2}$ cm^2 s^{-1}). This compels one to use the ideal gas model and it is the reason why the mixed Egelstaff and Schofield model could not be used when dealing with gas conditions.

A.5. Parameters

The relevant parameters used in the present calculations are summarized in table A.1 for the various systems. Symbols were defined in the previous sections.

In the case of hydrogens, indications concerning the possible use of a modified (few per cent higher) equilibrium distance R_{eq} to allow for better fits of the intramolecular part of the diffraction data has been sometimes reported [52]. However, the examples shown here (which never make use of fit procedures) were found to be insensitive to so fine an adjustment and, for this reason, the nominal values of table A.1 were anyway employed in the calculations concerning hydrogen and deuterium.

References

[1] Fermi E 1936 *Ric. Sci.* **7** 13
[2] Sachs R G and Teller E 1941 *Phys. Rev.* **60** 18
[3] Messiah A M L 1951 *Phys. Rev.* **84** 204
[4] Pope N K 1952 *Can. J. Phys.* **30** 597
[5] Zemach A C and Glauber R J 1956 *Phys. Rev.* **101** 118
Zemach A C and Glauber R J 1956 *Phys. Rev.* **101** 129
[6] Krieger T J and Nelkin M S 1957 *Phys. Rev.* **106** 290
[7] Rahman A 1961 *J. Nucl. Energy Reactor Sci.* A **13** 128
[8] Griffing G W 1961 *Phys. Rev.* **124** 1489
Griffing G W 1962 *Phys. Rev.* **127** 1179
[9] Young J A and Koppel J U 1964 *Phys. Rev.* A **135** 603
[10] Koppel J U and Young J A 1965 *Nukleonika* **8** 40
[11] Venkataraman G, Rao K R, Dasannacharya B A and Dayanidhi P K 1966 *Proc. Phys. Soc.* **89** 379
[12] Sinha S K and Venkataraman G 1966 *Phys. Rev.* **149** 1
[13] Sears V F 1966 *Can. J. Phys.* **44** 1279
Sears V F 1966 *Can. J. Phys.* **44** 1299
[14] Lurie N A 1967 *J. Chem. Phys.* **46** 352
[15] Sears V F 1967 *Can. J. Phys.* **45** 237
[16] Agrawal A K and Yip S 1969 *Nucl. Sci. Eng.* **37** 368
[17] Marshall W and Lovesey S W 1971 *Theory of Thermal Neutron Scattering* (Oxford: Clarendon)
[18] Egelstaff P A and Soper A K 1980 *Mol. Phys.* **40** 553
Egelstaff P A and Soper A K 1980 *Mol. Phys.* **40** 569
[19] Zoppi M 1993 *Physica* B **183** 235
[20] Zoppi M, Bafile U, Guarini E, Barocchi F, Magli R and Neumann M 1995 *Phys. Rev. Lett.* **75** 1779
[21] Guarini E, Barocchi F, Magli R, Bafile U and Bellissent-Funel M C 1995 *J. Phys.: Condens. Matter* **7** 5777
[22] Strauß G, Bassen A, Zweier H, Bertagnolli H, Tödheide K, Soper A K and Turner J 1996 *Phys. Rev.* E **53** 3505
[23] Guarini E, Bafile U, Barocchi F, Cilloco F and Magli R 1998 *Mol. Phys.* **94** 289
[24] Celli M, Magli R, Fischer H, Frommhold L and Barocchi F 1998 *Phys. Rev. Lett.* **81** 5828
[25] Celli M, Bafile U, Cuello G J, Formisano F, Guarini E, Magli R, Neumann M and Zoppi M 2002 in preparation
[26] Benmore C, Mos B, Egelstaff P and Verkerk P 1998 *J. Neutron Res.* **6** 279
[27] Benmore C J, Formisano F, Magli R, Bafile U, Verkerk P, Egelstaff P A and Barocchi F 1999 *J. Phys.: Condens. Matter* **11** 3091
[28] Guarini E, Casanova G, Bafile U and Barocchi F 1999 *Phys. Rev.* E **60** 6682
[29] Price D L and Sköld K 1987 *Methods of Experimental Physics* vol 23A (London: Academic) pp 1–97
[30] van Kranendonk J 1983 *Solid Hydrogen* (New York: Plenum)
[31] Ewing G E 1964 *J. Chem. Phys.* **40** 179
[32] Herzberg G 1945 *Molecular Spectra and Molecular Structure* vol 2 (Princeton, NJ: van Nostrand-Reinhold) pp 38–9
[33] Messiah A 1986 *Quantum Mechanics* vol 1 and 2 (Amsterdam: North-Holland)
[34] Gray C G and Gubbins K E 1984 *Theory of Molecular Fluids* (Oxford: Clarendon)
[35] Benmore C 1998 private communication
[36] Rosenthal J E 1934 *Phys. Rev.* **46** 730
[37] Egelstaff P A 1987 *Methods of Experimental Physics* vol 23B, ed K Sköld and e D Price (London: Academic) pp 405–70
[38] Placzek G 1952 *Phys. Rev.* **86** 377
[39] Magli R, Cilloco F and Guarini E 1999 unpublished
[40] Bermejo F J *et al* 1993 *Phys. Rev.* B **47** 15 097
Bermejo F J *et al* 1999 *Phys. Rev.* B **60** 15 154
Bermejo F J *et al* 2000 *Phys. Rev. Lett.* **84** 5359

[41] Bafile U, Celli M and Zoppi M 1996 *Physica* B **226** 304
[42] Randolph P D, Brugger R M, Strong K A and Schmunk R E 1961 *Phys. Rev.* **124** 460
[43] Harker Y D and Brugger R M 1965 *J. Chem. Phys.* **42** 275
[44] Dasannacharya B A and Venkataraman G 1967 *Phys. Rev.* **156** 196
[45] Webb F J 1967 *Proc. Phys. Soc.* **92** 912
[46] Egelstaff P A and Schofield P 1962 *Nucl. Sci. Eng.* **12** 260
[47] Copley J R D and Lovesey S W 1975 *Rep. Prog. Phys.* **38** 461
[48] Singwy K S and Sjölander A 1960 *Phys. Rev.* **120** 1093
Aamodt R, Case K M, Rosenbaum M and Zweifel P F 1962 *Phys. Rev.* **126** 1165
[49] Naghizadeh J and Rice S A 1962 *J. Chem. Phys.* **36** 2710
[50] Gradshteyn I S and Ryzhik I M 1994 *Table of Integrals, Series, and Products* ed A Jeffrey (London: Academic) ch 8
[51] Bartell L S, Kuchitsu K and deNeui R J 1961 *J. Chem. Phys.* **35** 1211
[52] Zoppi M, Soper A K, Magli R, Barocchi F, Bafile U and Aschcroft N W 1996 *Phys. Rev.* E **54** 2773